J. metamorphic Geol., 1999, **17**, 195–209

Application of K-feldspar–jadeite–quartz barometry to eclogite facies metagranites and metapelites in the Sesia Lanzo Zone (Western Alps, Italy)*

P. TROPPER,[1] E. J. ESSENE,[1,2] Z. D. SHARP[2,3] AND J. C. HUNZIKER[2]
[1]*Department of Geological Sciences, University of Michigan, Ann Arbor, MI 48109-1063, USA (e-mail: ptropper@umich.edu*
[2]*Institut de Minéralogie et Pétrographie, Université de Lausanne, BFSH-2, CH-1015 Lausanne, Switzerland*
[3]*Department of Geology, University of New Mexico, Albuquerque, NM 87131, USA.*

ABSTRACT The eclogite facies assemblage K-feldspar–jadeite–quartz in metagranites and metapelites from the Sesia-Lanzo Zone (Western Alps, Italy) records the equilibration pressure by dilution of the reaction jadeite + quartz = albite. The metapelites show partial transformation from a pre-Alpine assemblage of garnet ($Alm_{63}Prp_{26}Grs_{10}$)–K-feldspar–plagioclase–biotite ± sillimanite to the Eo-Alpine high-pressure assemblage garnet ($Alm_{50}Prp_{14}Grs_{35}$)–jadeite ($Jd_{80-97}Di_{0-4}Hd_{0-8}Acm_{0-7}$)–zoisite–phengite. Plagioclase is replaced by jadeite–zoisite–kyanite–K-feldspar–quartz, and biotite is replaced by garnet–phengite or omphacite–kyanite–phengite. Equilibrium was attained only in local domains in the metapelites and therefore the K-feldspar–jadeite–quartz (KJQ) barometer was applied only to the plagioclase pseudomorphs and K-feldspar domains. The albite content of K-feldspar ranges from 4 to 11 mol% in less equilibrated assemblages from Val Savenca and from 4 to 7 mol% in the partially equilibrated samples from Monte Mucrone and the equilibrated samples from Montestrutto and Tavagnasco. Thermodynamic calculations on the stability of the assemblage K-feldspar–jadeite–quartz using available mixing data for K-feldspar and pyroxene indicate pressures of 15–21 kbar (± 1.6–1.9 kbar) at 550 ± 50 °C. This barometer yields direct pressure estimates in high-pressure rocks where pressures are seldom otherwise fixed, although it is sensitive to analytical precision and the choice of thermodynamic mixing model for K-feldspar. Moreover, the KJQ barometer is independent of the ratio P_{H_2O}/P_T. The inferred limiting $a(H_2O)$ for the assemblage jadeite–kyanite in the metapelites from Val Savenca is low and varies from 0.2 to 0.6.

Key words: Eo-Alpine high pressure metamorphism; K-feldspar activity models; order-disorder; Western Alps.

INTRODUCTION

Despite much effort, few barometers have been developed that directly fix the pressures of eclogites (Essene, 1989). Solid–solid reactions, such as the equilibria:

$$\text{jadeite} + \text{quartz} = \text{albite} \quad (1)$$

$$\text{coesite} = \text{quartz} \quad (2)$$

$$\text{diamond} = \text{graphite} \quad (3)$$

(Eq. 1: Liu & Bohlen, 1995; Eq. 2: Bohlen & Boettcher, 1982; Eq. 3: Kennedy & Kennedy, 1976) seldom provide other than limiting information, because full equilibrium assemblages are rare in most rocks. Manning & Bohlen (1991) investigated applications of several solid–solid equilibria involving titanite and rutile to eclogites, but these reactions usually only provide limiting pressures because titanite forms only as late overgrowths on rutile in most eclogitic rocks. Dehydration reactions, such as:

$$\text{paragonite} = \text{jadeite} + \text{kyanite} + H_2O \quad (4)$$

$$\text{lawsonite} = \text{zoisite} + \text{kyanite} + \text{quartz} + H_2O \quad (5)$$

$$\text{phengite} = \text{K-feldspar} + \text{phlogopite} + \text{quartz} + H_2O \quad (6)$$

(Eq. 4: Holland, 1979a; Eq. 5: Newton & Kennedy, 1963; Eq. 6: Massonne & Schreyer, 1987) have been used to estimate or constrain the pressures of crustal eclogites and associated rocks (Holland, 1979a,b; Barnicoat & Fry, 1986; Koons, 1986; Newton, 1986; Massonne & Schreyer 1987; Barnicoat & Fry, 1989; Klemd, 1989; Massonne & Chopin, 1989; Jamtveit *et al.*, 1990). These applications require knowledge of the ratio P_{H_2O}/P_T or the often unstated assumption that $P_{H_2O} = P_T$. While it has been argued that crustal eclogites equilibrated at high H_2O pressures (e.g. Essene & Fyfe, 1967; Holland, 1979a,b; Barnicoat &

*Contribution No. 509 from the Mineralogical Laboratory, University of Michigan.

Fry, 1986; Evans, 1990), it has also been concluded that fluid-absent or water-diluted conditions (i.e. $P_{H_2O} < P_T$) prevail during the formation of most crustal eclogites (e.g. Fry & Fyfe, 1969; Essene *et al.*, 1970; Essene, 1989). Available experiments on the amphibolite–eclogite transition with tholeiitic basalts by Liu *et al.* (1996) suggest that the assemblage garnet + clinopyroxene forms at 22–16 kbar for $P_{H_2O} = P_T$ at temperatures from 700–900 °C, indicating that eclogites which formed at $T < 700$ °C and $P < 22$ kbar require $P_{H_2O} < P_T$. Significant dilution of H_2O by other fluid species has also been postulated during eclogite formation, that is $P_{H_2O} < P_T = P_T$ (e.g. NaCl: Fry & Fyfe, 1971; Andersen *et al.*, 1989; CO_2: Miller, 1974; Jamtveit *et al.*, 1990; N_2: Andersen *et al.*, 1989, 1993). Although paragonite and/or phengite are often found as accessory phases in crustal eclogites (Ahn *et al.*, 1985), textural evidence for equilibrium with garnet and omphacite is often equivocal. The baric stability of paragonite is highly sensitive to the ratio P_{H_2O}/P_T. If precise total pressures could be independently established by solid–solid equilibria, reaction (4) might be useful in constraining P_{H_2O} if it could be documented that paragonite equilibrated with the eclogite facies assemblage near its baric maximum (e.g. Wall & Essene, 1972; Holland, 1979a).

Many petrologists have obtained estimates of minimum pressures in plagioclase-free eclogites by combination of reaction (1) with K_D (Mg/Fe^{2+}) exchange thermometry of garnet and omphacite. Unfortunately, calibrations of this thermometer (e.g. Ellis & Green, 1979; Powell, 1985; Krogh, 1988; Pattison & Newton, 1989; Green & Adam, 1991; Ai, 1994) may be in error for most crustal eclogites, as the consequence of cation ordering in omphacite (Essene, 1982; Koons, 1984; Carpenter & Putnis, 1986; Essene, 1989), and the influence of high jadeite and grossular contents on the K_D remains unevaluated (Ganguly *et al.*, 1996). Identification of additional thermobarometers applicable to eclogites is clearly important for a better understanding of the depths at which they formed.

Sharp *et al.* (1992) applied reaction (1) to obtain pressures on an unusual coesite–sanidine grospydite xenolith of mantle origin. Their calculations relied on correcting reaction (1) for the reduced activity of albite in K-feldspar solid solution and of jadeite in pyroxene solid solution. Crustal eclogite facies rocks that contain Na-pyroxene with quartz and K-feldspar may be exploited with the same approach, which was the impetus for this contribution.

GEOLOGICAL SETTING

High-pressure metamorphic assemblages in metagranitic massifs of the Western Alps were first described by Lefévre & Michard (1965), Dal Piaz *et al.* (1972) and Compagnoni & Maffeo (1973). Subsequent workers have described K-feldspar-bearing eclogitic rocks in the Western Alps (Droop *et al.*, 1990; Le Goff & Ballevre, 1990; Biino & Compagnoni, 1992; Compagnoni *et al.*, 1995). Some of the K-feldspar–jadeite–quartz-bearing rocks have been described from one of the internal units of the Western Alps, the Sesia-Lanzo Zone. Compagnoni & Maffeo (1973) were the first to describe the metagranites from Monte Mucrone, which show a partial transformation from a pre-Alpine igneous assemblage to an Eo-Alpine high-pressure assemblage. Barbero (1992) and Venturini *et al.* (1994) described similar features in metapelites from Val Savenca. In addition to these rocks, which show only partial equilibration under Eo-Alpine high pressures, completely equilibrated metagranites can also be found in the Sesia-Lanzo Zone, in the Aosta Valley, near Montestrutto and Tavagnasco. Since the temperature of the Eo-Alpine high-pressure metamorphism in the Western Alps is much better constrained than the pressures, these metagranites and metapelites from the Sesia-Lanzo Zone provide an excellent opportunity to estimate the pressures, based on the assemblage K-feldspar–jadeite–quartz.

The Sesia-Lanzo Zone is one of the internal Austro-alpine units of the Western Alps in Northern Italy (Compagnoni *et al.*, 1977). Based on petrographic and structural investigations, it is subdivided into three main complexes (Venturini *et al.*, 1994; Venturini, 1995). The first, the Polymorphic Basement Complex, corresponding to the lower unit of the Sesia-Lanzo Zone after Compagnoni *et al.* (1977), is further subdivided, based on detailed mapping of the central Sesia-Lanzo Zone, into an internal, an intermediate and an external unit. The internal unit in the eastern part is equilibrated under eclogite facies conditions and contains mostly eclogites and blueschists and rarely metagranites and metapelites (Dal Piaz *et al.*, 1972). Towards the west, the intermediate unit occurs, characterized by partial greenschist facies overprint, and then the external unit with a pervasive greenschist facies overprint. The second main complex, the Monometamorphic Cover Complex, is thought to be an autochthonous cover of the Sesia-Lanzo Zone. The third main complex, the pre-Alpine high temperature Basement Complex ('Seconda Zona Dioritica-Kinzigitica' or IIDK), comprises Hercynian high-temperature basement rocks and is located between the internal and external parts of the Polymetamorphic Basement Complex.

Permian granites of Monte Mucrone, pre-Alpine metagranites of Montestrutto and metapelites of Val Savenca occur in the Polymetamorphic Basement Complex of the Sesia-Lanzo Zone and were metamorphosed during an Eo-Alpine event (Dal Piaz *et al.*, 1972; Oberhänsli *et al.*, 1985). The metagranites and metapelites now contain an assemblage (K-feldspar–jadeite–zoisite–phengite–quartz ± kyanite) which replaced igneous and metamorphic plagioclase, along with garnet coronas around relict igneous or metamorphic titanian biotite (Dal Piaz *et al.*, 1972; Compagnoni & Maffeo, 1973; Oberhänsli *et al.*, 1985; Hy, 1984; Früh-Green, 1987; Koons *et al.*, 1987; Pognante *et al.*, 1987; Barbero, 1992; Venturini *et al.*, 1994). Because of the partial transformation, only local equilibrium has been achieved. With increasing recrystallization, omphacitic pyroxene forms in these rocks by reaction with components from zoisite, jadeite, quartz and residual biotite.

The temperature range for the high-pressure metamorphism in the Sesia-Lanzo Zone is 500–600 °C, with results calculated using a variety of geothermometers clustering around 550 °C (Morten, 1993). Textural evidence in the partially re-equilibrated metapelites from Val Savenca shows that omphacitic pyroxene grew in different domains than jadeite and sometimes formed rims around jadeite. Temperature estimates from partially and fully re-equilibrated rocks from Val Savenca obtained with garnet–omphacite thermometry are 600 ± 50 °C for peak temperature (Krogh, 1988; Ai 1994). These temperatures are comparable to the estimates by Hy (1984) and somewhat higher than most estimates which might be due to small-scale variations in Mg/Fe^{2+} ratios in garnet, which are the result of partial equilibration. The temperatures obtained from garnet–jadeite pairs from a partially re-equilibrated rock of the same locality yield 800–900 °C and are obviously erroneous. This is probably due to the lack of data on the influence of high jadeite contents on the $K_D(Mg/Fe^{2+})$ (Ganguly *et al.*, 1996).

TEXTURAL RELATIONS AND PETROGRAPHY

Samples of metagranites were collected from Monte Mucrone and Monte Mars, 10 km west of Biella in

western Italy. Similar assemblages were found to the south-west at Montestrutto and Tavagnasco, 7 km north of Ivrea. The metapelite samples were collected from Val Savenca, 20 km south-west of Ivrea, where exceptionally well preserved relicts of pre-Alpine garnet–sillimanite–biotite–quartz ± K-feldspar gneisses have been found (Barbero, 1992; Venturini *et al*., 1994). Examination of thin sections from Monte Mucrone revealed textures similar to those described previously (Dal Piaz *et al*., 1972; Compagnoni & Maffeo, 1973; Hy, 1984; Oberhänsli *et al*., 1985; Koons *et al*., 1987). Back-scattered electron (BSE) images were obtained with the University of Michigan Hitachi scanning electron microscope (SEM) to illustrate key textures (Figs 1a–d, 2a–d). In the samples from Monte Mucrone, former igneous plagioclase is replaced by fine intergrowths of jadeite, quartz and minor K-feldspar cut by fine blades of zoisite (Fig. 1a), and former igneous orthoclase is replaced by homogeneous K-feldspar that touches areas containing quartz and jadeite (Fig. 1b).

The textures at Val Savenca are similar to those found in the Monte Mucrone metagranites, except that kyanite appears in the plagioclase porphyroblasts (Fig. 1c) and garnet is part of the pre-Alpine assemblage. Relict garnet (Grt I) contains abundant biotite and quartz inclusions and reacts with the coexisting plagioclase and biotite to form inclusion-rich (kyanite, clinopyroxene, quartz, rutile inclusions) reaction rims (Grt II) towards the plagioclase pseudomorph (Fig. 1d). In both locations, relict igneous or metamorphic biotite is rimmed by a thin rind of garnet (Fig. 1d). The replacement of plagioclase by jadeite–zoisite–kyanite–quartz takes place also along former fractures and inclusions in garnet. Within the jadeite–zoisite–kyanite–K-feldspar pseudomorphs after plagioclase, jadeite and quartz coexist with K-feldspar (Fig. 2a).

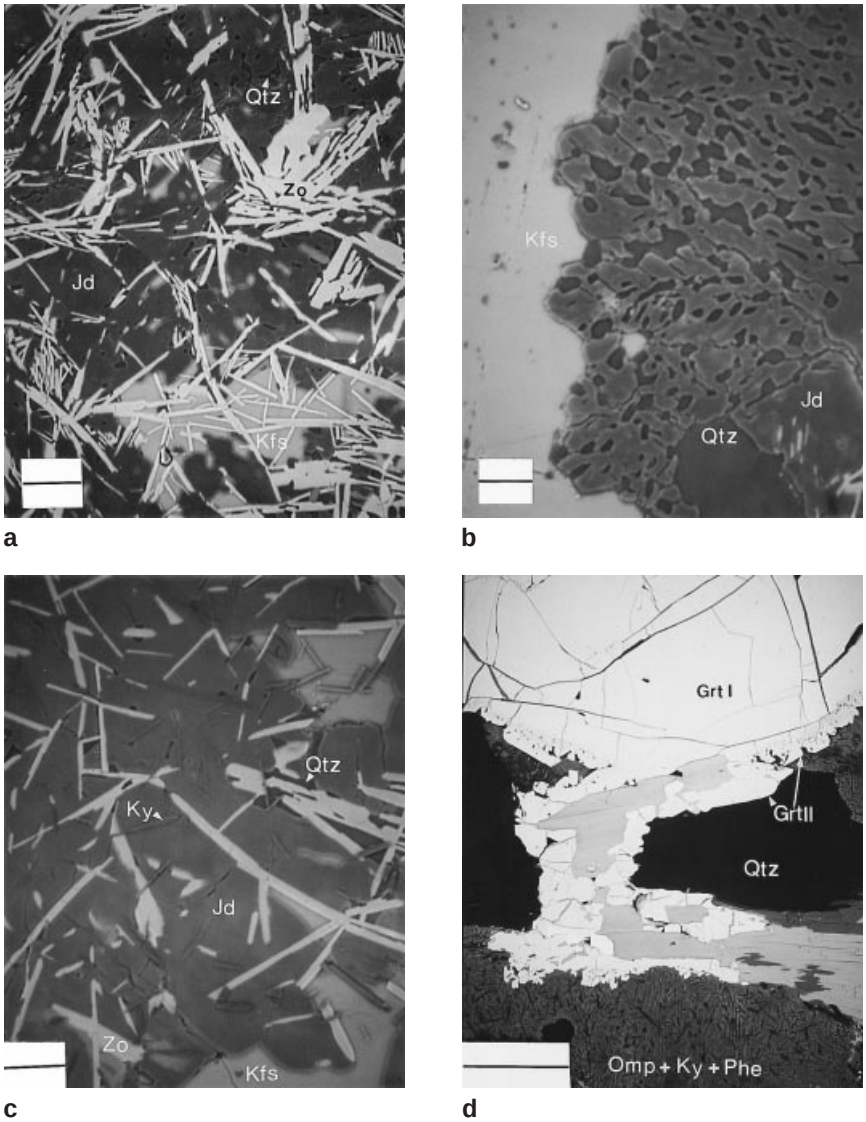

Fig. 1. (a) BSE image of jadeite (Jd)–zoisite (Zo)–quartz (Qtz) ± K-feldspar (Kfs) pseudomorph after relict granitic plagioclase (sample MC 1, Monte Mucrone); scale bar = 10 μm. (b) BSE image of homogeneous K-feldspar (Kfs) touching jadeite (Jd) and quartz (Qtz) (sample MC 2, Monte Mucrone); scale bar = 10 μm. (c) BSE image of jadeite (Jd)–kyanite (Ky)–zoisite (Zo)–K-feldspar (Kfs)–quartz (Qtz) ± muscovite replacing relict metamorphic plagioclase (sample VS 8, Val Savenca); scale bar = 10 μm. (d) BSE image of pre-Alpine garnet (Grt I) and Alpine garnet (Grt II). Garnet II has grown around relict biotite and at the expense of coexisting former plagioclase, which is now replaced by jadeite/omphacite–kyanite–phengite (sample VS 8, Val Savenca); scale bar = 100 μm. All abbreviations are according to Kretz (1983).

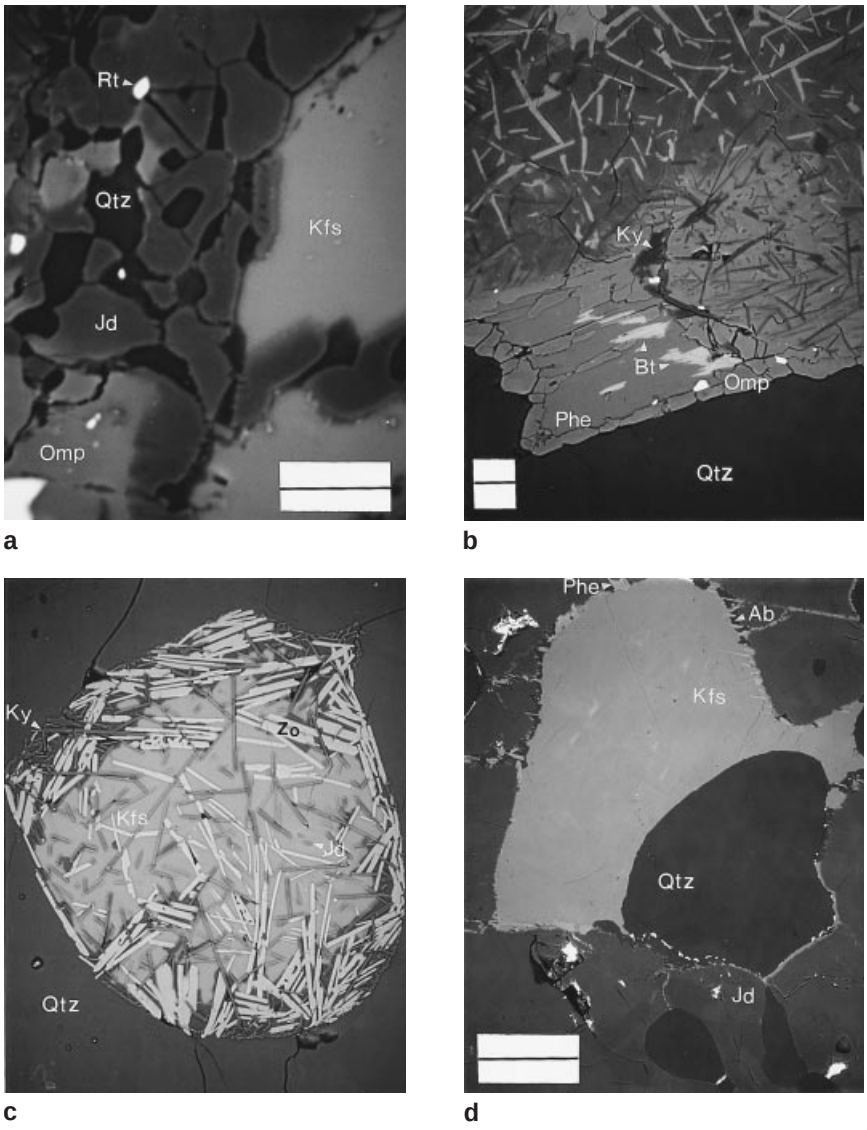

Fig. 2. (a) BSE image of the core of a pseudomorph with coexisting jadeite (Jd)–K-feldspar (Kfs)–quartz (Qtz), jadeite also shows replacement by omphacite (Omp). Jadeite contains rutile (Rt) inclusions; (sample MC 1, Monte Mucrone); scale bar = 10 μm. (b) BSE image of phengite (Phe)–omphacite (Omp)–kyanite (Ky) replacing pre-Alpine relict metamorphic biotite (Bt) coexisting with former plagioclase, which is replaced in the upper part of the figure by the assemblage zoisite + jadeite + K-feldspar + kyanite + quartz (sample VS 8, Val Savenca). The omphacitic areas contain no zoisite and the dark matrix on the bottom of the figure is quartz (Qtz); scale bar = 10 μm. (c) BSE image of recrystallized K-feldspar (Kfs) with abundant zoisite (Zo), kyanite (Ky) $\pm$ quartz (Qtz) inclusions and a few jadeite (Jd) inclusions. The abundance of kyanite (Ky) and quartz (Qtz) increases in the rims of the K-feldspar (sample VS 31, Val Savenca); scale bar = 10 μm. (d) BSE image of a metagranitic sample containing a coarse-grained jadeite (Jd) porphyroblast with K-feldspar (Kfs) and quartz (Qtz) inclusions (sample MS 2, Montestrutto). The K-feldspar is rimmed by phengitic white mica (Phe) and albite (Ab); scale bar = 100 μm. All abbreviations are according to Kretz (1983).

Jadeite also shows some late-stage replacement by omphacite at the rims (Fig. 2a). Biotite is replaced by the assemblage phengite–omphacite–kyanite if it is adjacent to former plagioclase (Fig. 2b), otherwise by phengite–rutile/titanite, or only by phengite. These omphacitic areas contain no zoisite (Fig. 2b). Former metamorphic K-feldspar seems to recrystallize during Alpine metamorphism, as suggested by development of a homogeneous host with included needles of zoisite and jadeite (Fig. 2c). Sometimes quartz- and kyanite-rich areas form at the rims of K-feldspar porphyroblasts (Fig. 2c). More recrystallized samples contain omphacite, coarse inclusion-rich garnet (kyanite, quartz, zoisite inclusions in the core, omphacite inclusions at the rim), phengite, paragonite and Na–Ca amphibole (barroisite).

The samples from Montestrutto and Tavagnasco show complete re-equilibration under Eo-Alpine high-pressure conditions and contain coarse-grained jadeite porphyroblasts with abundant K-feldspar and quartz inclusions (Fig. 2d) in a matrix of K-feldspar–white mica–quartz. Large K-feldspar porphyroblasts are rimmed by albite and phengite, due to later retrogression.

ANALYTICAL DATA

Electron microprobe analyses (EMPA) were obtained on minerals of the important assemblages using the Cameca CAMEBAX electron microprobe at the University of Michigan. Analysis were obtained at 15 kV and 10 nA with a point beam, except for feldspars and micas which were analysed with a 3 μm square beam to minimize volatilization. Due to the size and the nature of the plagioclase pseudomorphs, the jadeite in the plagioclase pseudomorphs was analysed with 10 kV and 10 nA to minimize any contamination from adjacent minerals. Natural and synthetic mineral standards were used and the raw data were reduced with a PAP-type correction provided by Cameca. Analytical standards include Tiburon albite (Na), Gotthard adularia (K), New Idria jadeite (Na), natural diopside (Si), Broken Hill rhodonite (Mn), synthetic uvarovite (Cr), Ingamells almandine (Fe, Al), synthetic geikelite (Ti), Marjalahti

olivine (Mg), natural sanbornite (Ba), Topaz Mts topaz (F) and Willsboro wollastonite (Ca). Formulae were calculated with the program MINFILE (Afifi & Essene, 1988). Analytical totals and stoichiometries are judged to be acceptable.

The compositions of K-feldspar (Table 1) are similar to those reported by Oberhänsli *et al.* (1985) with only minor Ba and Ca substitution. They plot essentially on the albite–K-feldspar binary (Fig. 3a) and therefore may be considered as binary solids for the purpose of phase equilibrium calculations. The albite content (Ab_{4-7}) is uniform in most of the samples, although some variation occurs in the partially equilibrated samples from Val Savenca (Ab_4 to Ab_{11}). The high albite contents are from small K-feldspar inclusions in jadeite without coexisting quartz.

The structural state of the K-feldspar in the metagranites and metapelites is important for calculation of the mixing parameters of the feldspar. Powder X-ray diffraction was used to obtain information on the structural states of the Eo-Alpine K-feldspar. K-feldspar was separated from metagranite samples from Montestrutto (sample MS 1), Tavagnasco (sample TA 2) and Monte Mucrone (sample MC 1). They were X-rayed on a SCINTAG powder diffractometer with silicon as an internal standard. A least-squares refinement of the unit cell dimensions was obtained from the powder patterns (Table 2). These were used to estimate the structural states and compositions of the K-feldspar (Stewart & Wright, 1974; Kroll & Ribbe, 1983; Hovis, 1986). The mole fractions of $KAlSi_3O_8$ obtained from the unit cell data (0.95–0.97) with the method described by Hovis (1986) show somewhat more Kfs content than data obtained by electron microprobe analysis (0.91–0.96). The order parameter Z describes the Al–Si distribution between the two different tetrahedral T1 and T2 sites (Thompson, 1969). The X-ray data indicate that the sample from Tavagnasco metagranite is nearly pure microcline and highly ordered with a Z of 0.97, and K-feldspar from Monte Mucrone and Montestrutto metagranites show some disorder with a Z of 0.83 and 0.85 (Table 2).

Following Essene & Fyfe (1967), the pyroxene analyses (Table 3) have been plotted on an acmite–(diopside + hedenbergite)–jadeite diagram (Fig. 3b). Early-formed pyroxene shows high jadeite contents, about 80–97 mol% $NaAlSi_2O_6$, and later replacements are omphacitic with 40–50 mol% $NaAlSi_2O_6$. There is essentially no Ti, Cr and Mn, and some excess Al in jadeite, similar to the analyses reported by Koons *et al.* (1987). This leads to very low calculated acmite contents, which are zero in many cases (Fig. 3b). Most compositions plot very close to the jadeite end-member composition with (Di + Hd) < 0.2. The omphacites show no acmite content and (Di + Hd) ranges between 0.5 and 0.75 (Fig. 3b).

The garnet compositions (Table 4) are plotted on a triangular diagram with the components almandine, grossular and pyrope (Fig. 4). Due to the domainal equilibrium, the garnet from Val Savenca shows a wide range in composition. The pre-Alpine garnet cores are homogeneous and are mostly pyrope–almandine-rich solid solutions ($Alm_{63}Prp_{26}Grs_{10}$). Newly grown garnet rims adjacent to jadeite-rich domains are more calcic ($Alm_{50}Prp_{14}Grs_{35}$) than garnet rims coexisting with omphacite ($Alm_{61}Prp_{19}Grs_{21}$) and garnet rimming biotite ($Alm_{69}Prp_{21}Grs_{10}$). This trend towards Ca-rich compositions can be seen in Fig. 4 and is comparable to the observations of Koons (1984), who pointed out that pyroxene coexisting with garnet becomes more Fe-rich with increasing jadeite content and the garnet less Fe-rich.

The white mica contains 6.0–6.7 Si per formula unit and those replacing former biotite show high Ti contents (Table 5). The relict biotite contains up to 0.6 wt% F (Table 5) and charge balance considerations require some OH to be replaced by O, indicating coupled substitutions such as $TiO_2 <=> Mg(OH)_2 <=> AlOOH$ (Bohlen *et al.*, 1980). The zoisites are nearly pure $Ca_2Al_3Si_3O_{12}(OH)$ with only 0–3 mol% pistacite component, although more recrystallized samples contain more iron-rich epidote (Table 6). Titanite contains minor amounts of Al and F, due to the coupled substitution Al + (F,OH) <=> Ti + O.

THERMODYNAMIC CALCULATIONS

Solid solution models and calculated *P–T* data

In order to calculate the shift in reaction (1) for dilution of albite by K-feldspar and of jadeite by diopside, it is necessary to use solution models that are applicable to the structural states involved and appropriate for the temperatures (500–600 °C) at which the phases equilibrated.

Hovis (1988) and Hovis *et al.* (1991) performed K–Na exchange experiments to obtain Gibbs energies and entropies of mixing for feldspar series with different degrees of Si–Al disorder. They calculated two sets of Margules parameters for the disordered analbite–sanidine series based on the extraction of parameters from reversed solvus experiments (referred to here as

Table 1. Representative electron microprobe analyses of K-feldspar[a].

	1	2	3	4	5	6	7	8	9
SiO_2	62.85	63.27	64.32	64.84	63.08	64.06	64.28	64.83	64.81
Al_2O_3	18.75	18.47	18.35	18.63	18.76	18.73	19.33	18.39	18.71
Fe_2O_3	0.22	n.d.	n.d.	n.d.	0.07	0.03	0.02	0.09	0.05
MgO	n.d.	n.d.	n.d.	n.d.	0.02	0.02	n.d.	n.d.	n.d.
CaO	n.d.	0.01	n.d.	n.d.	n.d.	n.d.	0.12	0.08	n.d.
BaO	1.74	1.07	0.08	n.d.	1.13	0.90	0.64	0.37	0.53
K_2O	15.37	15.68	16.41	16.31	15.48	15.71	14.19	16.19	15.97
Na_2O	0.61	0.77	0.42	0.47	0.80	0.55	1.13	0.48	0.46
$\sum$	99.54	99.27	99.57	100.25	99.33	99.98	99.70	100.42	100.66
Si	2.96	2.97	2.99	2.99	2.96	2.98	2.97	2.99	2.99
Al	1.04	1.02	1.01	1.01	1.04	1.03	1.05	1.00	1.01
Fe^{3+}	0.01	n.d.	n.d.	n.d.	<0.01	<0.01	<0.01	<0.01	<0.01
Ba	0.03	0.02	<0.01	n.d.	0.02	0.02	0.01	0.01	0.01
Mg	n.d.	n.d.	n.d.	n.d.	<0.01	<0.01	n.d.	n.d.	n.d.
Ca	n.d.	n.d.	n.d.	n.d.	n.d.	n.d.	0.01	<0.01	n.d.
K	0.92	0.94	0.97	0.96	0.93	0.93	0.84	0.95	0.94
Na	0.06	0.07	0.04	0.04	0.07	0.05	0.10	0.04	0.04
$\sum$ cations	5.01	5.02	5.01	5.00	5.02	5.00	4.97	5.00	5.00
X_{Ab}	0.06	0.07	0.04	0.04	0.07	0.05	0.11	0.04	0.04
X_{Kfs}	0.91	0.91	0.96	0.96	0.91	0.93	0.88	0.95	0.95
X_{Cs}	0.03	0.02	n.d.	n.d.	0.02	0.02	0.01	0.01	0.01

[a] Formulae normalized to 8 oxygens; n.d., not detected. X_{Ab}: [Na/(Na + K + Ba)], X_{Kfs}: [K/(Na + K + Ba)], X_{Cs}: [Ba/(Na + K + Ba)]. K-feldspar analyses from Monte Mucrone sample MC 1 [nos. 1 and 2]; Montestrutto sample MS 1 [no. 3]; Tavagnasco sample TA 1 [no. 4]; Val Savenca samples VS 8 [nos. 5, 6 and 7] and sample VS 27 [nos. 8 and 9].

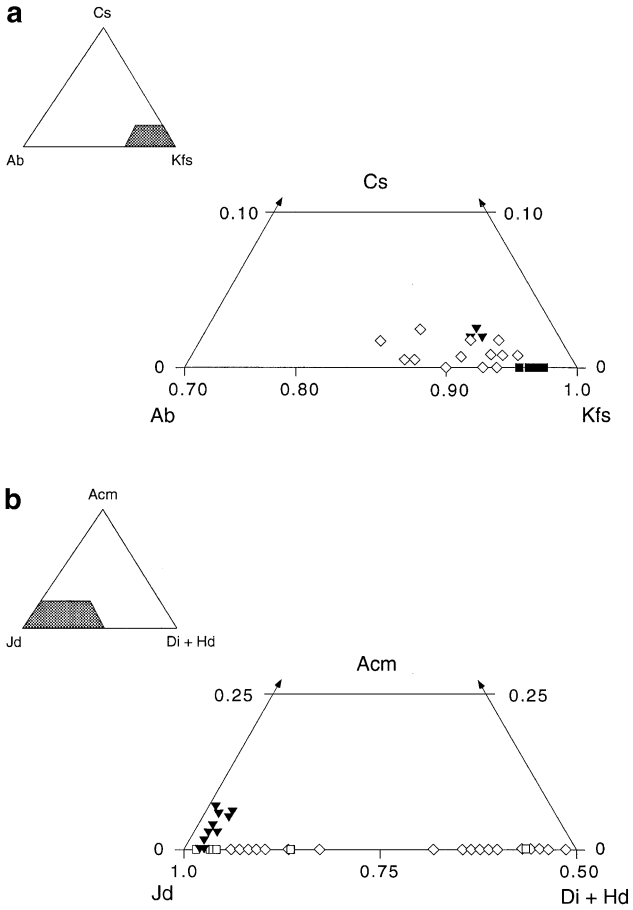

Fig. 3. (a) Composition of feldspar from this study (◇: Val Savenca; ▼: Tavagnasco and Montestrutto; ■: Monte Mucrone) shown in an albite (Ab)–K-feldspar (Kfs)–celsian (Cs) diagram. (b) Composition of pyroxene from this study shown in an Acm–(Di+Hd)–Jd diagram (Essene & Fyfe, 1967). Acm, acmite; Di, diopside; Hd, hedenbergite; Jd, jadeite ◇: Val Savenca; □: Monte Mucrone; ▼: Montestrutto Tavagnasco. Calculation of the pyroxene components after Essene & Fyfe (1967): Acm = Na–Al; Jd = Al; (Di + Hd) = Ca.

model H1) and their ion-exchange experiments and solution calorimetric measurements (referred to here as model H2). The Margules parameters for both models of disordered K-feldspar are listed in Table 7 and the activity calculations are listed in Appendix 1. The calculated a–X relations for model H1 are strongly non-ideal and since there is a solvus between analbite and sanidine, the activities are >1 for X(Kfs) compositions, which lie inside the solvus (Fig. 5a). The a–X relations also show a strong pressure dependency (Fig. 5b).

Since XRD data show that K-feldspar is highly ordered, it is also necessary to evaluate mixing models for the ordered low microcline–low albite modifications. Bachinski & Müller (1971) generated mixing parameters from the locus of the solvus for ordered alkali feldspars (Table 7), based on homogenization and ion-exchange experiments on the low albite–low microcline solvus in the temperature range 650–900 °C. Even though their experiments were performed at temperatures where ordered alkali feldspars are metastable with respect to more disordered equivalents, the rates of disordering of initially ordered feldspar were sufficiently sluggish that the metastable solvus for low albite–low microcline was apparently obtained. These data may be used to calculate a–X relations for microcline and albite solid solutions at temperatures >450–500 °C. Use of their data must be regarded as tentative for two reasons: (1) their experiments were carried out at 650–900 °C and extrapolation to lower temperatures might produce large uncertainties, and (2) some of the experiments produced conflicting results and inconclusive reaction directions, probably resulting from short run durations. A different thermodynamic treatment of K-feldspar is applied by Carpenter & Salje (1994). They applied Landau theory to describe the thermodynamics of cation-ordering in K-feldspar and the resulting change of thermodynamic excess parameters such as H^{ex}, S^{ex} and G^{ex}, but unfortunately no mixing parameters have been generated for K-feldspar solid solutions.

The nature of the monoclinic–triclinic transition is still a matter of debate. Brown & Parsons (1989) reviewed the experimental data on ordering in alkali feldspar and proposed that the degree of order in K-feldspar varies strongly and continuously with temperatures below 500–525 °C. In contrast, Kroll *et al.* (1991) and Carpenter & Salje (1994) favoured a first-order transition with a significant jump in equilibrium degree of order. A transition temperature of 450–500 °C is generally accepted (e.g. Kroll *et al.*, 1991). Figure 6 shows the calculated solvi and critical temperatures for the three models at 15 kbar. In light of the accepted transition temperature, it is likely that the K-feldspar in the Eo-Alpine metagranites

Table 2. Unit cell parameters of K-feldspar.

Sample	a	b	c	α	β	γ	Al(T1)	Al(T2)	*Z*	X_{Kfs}[a]	X_{Kfs}[b]
Tavagnasco	8.577	12.971	7.223	90.591	116.004	87.667	0.492	0.010	0.968	0.966	0.958
±1σ	0.007	0.005	0.004	0.054	0.046	0.056	0.004	0.004	0.072	0.011	0.002
Montestrutto	8.579	12.956	7.217	90.570	115.934	87.673	0.461	0.039	0.848	0.971	0.961
±1σ	0.007	0.008	0.005	0.102	0.077	0.099	0.004	0.004	0.090	0.011	0.002
Monte Mucrone	8.574	12.955	7.216	90.037	116.014	89.341	0.461	0.039	0.833	0.957	0.912
±1σ	0.001	0.001	0.001	0.009	0.015	0.021	0.004	0.004	0.018	<0.001	0.002

Samples: Tavagnasco TA 1, Montestrutto MS 1, Monte Mucrone MC 1; unit cell parameters (a, b, c, α, β, γ) of triclinic K-feldspars from this study; Al (T1) and Al(T2) mole fractions of Al in tetrahedral sites T1 and T2; *Z*, ordering parameter (Hovis, 1986). [a] calculated from XRD data after Hovis (1986); [b] calculated from electron microprobe analyses.

Table 3. Representative electron microprobe analyses of pyroxene[a].

	1	2	3	4	5	6	7	8	9
SiO_2	58.96	58.93	60.02	58.68	56.22	58.02	55.86	58.47	56.23
TiO_2	0.04	0.02	0.01	n.d.	0.10	0.01	0.12	0.01	0.19
Al_2O_3	24.88	23.19	25.41	23.91	13.64	23.15	14.98	22.68	13.60
Cr_2O_3	n.d.	0.01	0.02	n.d.	n.d.	n.d.	0.03	0.07	0.08
Fe_2O_3	0.10	n.d.	n.d.	n.d.	n.d.	n.d.	n.d.	n.d.	n.d.
FeO	1.34	2.14	0.10	1.71	4.33	2.30	4.74	2.64	4.96
MnO	n.d.	0.01	n.d.	n.d.	n.d.	n.d.	n.d.	0.01	0.04
MgO	0.04	0.09	n.d.	0.35	5.84	0.82	5.61	0.77	6.31
CaO	0.47	0.75	0.73	1.47	11.57	2.47	10.90	3.21	11.47
Na_2O	14.78	14.47	14.59	13.70	8.02	13.41	7.99	12.68	7.77
$\sum$	100.60	99.61	100.88	99.83	99.86	100.17	100.22	100.53	100.66
Si	1.99	2.01	2.00	2.00	1.99	1.98	1.97	1.99	1.98
$Al^{(IV)}$	0.01	n.d.	n.d.	n.d.	0.01	0.02	0.03	0.01	0.02
$Al^{(VI)}$	0.97	0.93	1.00	0.96	0.56	0.91	0.59	0.90	0.55
Ti	<0.01	n.d.	n.d.	n.d.	<0.01	n.d.	<0.01	n.d.	0.01
Fe^{3+}	<0.01	n.d.	n.d.	n.d.	n.d.	n.d.	n.d.	n.d.	n.d.
Fe^{2+}	0.04	0.06	<0.01	0.05	0.13	0.07	0.14	0.08	0.15
Cr	n.d.	n.d.	<0.01	n.d.	n.d.	n.d.	<0.01	<0.01	<0.01
Mn	n.d.	n.d.	n.d.	n.d.	n.d.	n.d.	n.d.	n.d.	<0.01
Mg	<0.01	0.01	n.d.	0.02	0.31	0.04	0.30	0.04	0.33
Ca	0.02	0.03	0.03	0.05	0.44	0.09	0.41	0.12	0.43
Na	0.97	0.96	0.94	0.90	0.55	0.89	0.55	0.84	0.53

[a] Formulae normalized to 4 cations; n.d., not detected. Jadeite analyses from Tavagnasco, sample TA 1 [no. 1] and from Montestrutto sample MS 1 [no. 2]. Pyroxene analyses from Monte Mucrone sample MC 1—jadeite [nos. 3 and 4] and omphacite [no. 5], and from Val Savenca samples VS 8—jadeite [no. 6], omphacite [no. 7]—and VS 27—jadeite [no. 8], omphacite [no. 9].

Table 4. Representative electron microprobe analyses of garnet[a].

	1	2	3	4	5	6	7	8	9
SiO_2	38.08	38.60	38.89	37.81	38.37	38.87	38.02	37.90	37.65
TiO_2	0.09	0.02	0.04	0.10	0.02	n.d.	0.06	0.08	0.19
Al_2O_3	21.51	21.47	21.55	21.84	21.91	21.54	21.27	21.32	21.10
Cr_2O_3	n.d.	n.d.	n.d.	0.05	0.02	0.01	0.05	n.d.	0.15
FeO	34.54	26.34	23.02	30.52	27.59	21.05	30.59	27.37	23.68
MnO	0.74	0.32	0.40	0.21	0.17	0.29	0.17	0.23	0.43
MgO	3.67	1.63	1.52	5.14	4.86	1.92	4.94	3.63	1.39
CaO	1.80	11.74	15.19	3.57	7.21	15.77	3.98	8.95	15.10
$\sum$	100.43	100.12	100.61	99.18	100.13	99.46	99.07	99.49	100.69
Si	3.02	3.04	3.03	2.99	3.00	3.00	2.98	3.00	2.98
Al	2.01	1.99	1.98	2.04	2.02	2.01	2.02	1.99	1.97
Ti	0.01	<0.01	<0.01	0.01	<0.01	n.d.	<0.01	0.01	0.01
Cr	n.d.	n.d.	n.d.	<0.01	<0.01	n.d.	n.d.	n.d.	0.01
Fe^{2+}	2.29	1.73	1.50	2.02	1.80	1.40	2.06	1.81	1.57
Mn	0.05	0.02	0.03	0.01	0.01	0.02	0.01	0.02	0.03
Mg	0.44	0.19	0.18	0.61	0.57	0.23	0.59	0.43	0.16
Ca	0.15	0.99	1.27	0.30	0.60	1.34	0.34	0.76	1.28
$\sum$ cations	7.97	7.96	7.98	7.98	7.99	7.99	8.00	8.00	8.02
X_{Alm}	0.78	0.59	0.50	0.69	0.60	0.47	0.68	0.60	0.52
X_{Prp}	0.15	0.07	0.06	0.20	0.19	0.08	0.20	0.14	0.05
X_{Grs}	0.05	0.33	0.43	0.10	0.20	0.44	0.11	0.25	0.42
X_{Sps}	0.02	0.01	0.01	0.01	0.01	0.01	0.01	0.01	0.01

[a] Formulae normalized to 12 oxygens; n.d. not detected. X_{Alm}: [Fe/(Fe + Mg + Ca + Mn)], X_{Prp}: [Mg/(Fe + Mg + Ca + Mn)], X_{Grs}: [Ca/(Fe + Mg + Ca + Mn)], X_{Sps}: [Mn/(Fe + Mg + Ca + Mn)]. Garnet rim analyses from Monte Mucrone sample MC 1—garnet growing around biotite [no. 1], garnet coexisting with jadeite [nos. 2 and 3]. Garnet rim analyses from Val Savenca sample VS 8—garnet growing around biotite [no. 4] and garnet coexisting with omphacite [no. 5] and jadeite [no. 6]. Garnet rim analysis from Val Savenca sample VS 31—garnet growing around biotite [no. 7], garnet coexisting with omphacite [no. 8] and jadeite [no. 9].

equilibrated as highly disordered modifications, but no information about the actual degree of disorder is preserved. As these samples cooled from the eclogite facies Eo-Alpine event, these feldspars became more ordered, which is indicated by microscopic cross-hatched twinning in some of the K-feldspar. On the other hand, the lower values of the order parameter Z (0.83 and 0.85, Table 6) for the samples from Monte Mucrone and Montestrutto indicate that there is still some disorder preserved in K-feldspar. The activities of K-feldspar and the shift in reaction (1) were calculated using the models for fully ordered microcline and fully disordered sanidine (Appendix 2). In the light of the accepted transition temperature of *c.* 450–500 °C, the model for disordered K-feldspar is preferentially used.

Most of the analysed K-feldspar contains minor Ba, and its effect on the thermodynamic calculations must be considered. However, Ba is only a minor substitution and it is treated here as an ideal diluent where $a(NaAlSi_3O_8)$ is multiplied by $(1–X_{Cs})$ to correct for the small mole fraction (< 0.03) of celsian.

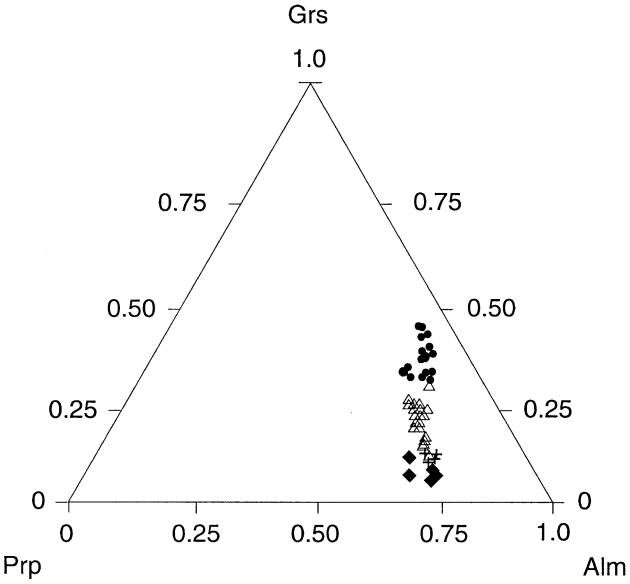

Fig. 4. Composition of garnet in an almandine (Alm)–grossular (Grs)–pyrope (Prp) diagram. The data are from partially re-equilibrated samples from Val Savenca ◆: pre-Alpine garnet; +: garnet coexisting with biotite; △: garnet coexisting with omphacite; ●: garnet coexisting with jadeite.

The structural state of sodic pyroxene is also dependent on composition as well as the temperature of equilibration. The order–disorder transition of $P2_1/n$ to C2/c omphacite has been located at 800–850 °C (Carpenter, 1981), well above the temperatures of the eclogite facies rocks in this study. In this paper, Holland's (1983, 1990) mixing parameters for a two-site simple reciprocal model are used for sodic pyroxenes (Table 7 and Appendix 1). Based on experiments with ordered omphacite involving dilution of reaction (1), Holland (1983) estimated a–X relations for pyroxene. Holland (1990) extended his calculations to the diopside–jadeite–acmite ternary, contouring the ternary for a–X relations at 500 °C. Although the experiments were conducted at 600 °C, extrapolation to lower temperatures will involve little error for nearly pure jadeite. On the other hand, calculations at 500 °C for omphacite with his data necessarily involve extrapolation and may have systematic errors, if omphacite forming at these temperatures is more fully ordered than that used in the experiments. Gasparik (1985) combined Holland's (1983) experiments with his own experimental data on this system at higher temperatures to obtain a mixing model consistent with the available experimental data. Gasparik's fit has doubtful extrapolative power because the ordering in

Table 5. Representative electron microprobe analyses of mica[a].

	1	2	3	4	5	6	7	8	9	10
SiO_2	38.96	38.14	38.61	38.46	49.07	48.92	48.57	48.67	48.83	48.25
TiO_2	5.69	6.16	5.52	5.42	2.92	0.11	2.70	1.98	0.25	0.41
Al_2O_3	13.57	13.38	15.06	14.57	25.32	27.25	28.30	28.21	29.23	29.12
Cr_2O_3	n.d.	n.d.	0.07	0.09	0.06	n.d.	0.06	0.08	n.d.	n.d.
Fe_2O_3	n.d.	n.d.	n.d.	n.d.	0.19	3.20	n.d.	1.45	0.86	1.37
FeO	17.18	17.62	15.22	15.52	2.59	0.44	2.22	0.91	3.87	3.72
MnO	0.04	0.09	0.01	0.04	n.d.	0.06	n.d.	0.03	0.09	0.18
MgO	9.86	9.63	10.64	11.10	3.32	3.27	2.41	2.92	0.92	0.76
CaO	n.d.	n.d.	n.d.	n.d.	0.01	n.d.	0.12	n.d.	n.d.	n.d.
BaO	0.28	0.30	0.24	0.14	0.45	1.39	0.36	0.13	0.03	0.01
Na_2O	0.02	0.03	n.d.	0.01	0.09	0.13	0.09	0.07	0.17	0.04
K_2O	9.95	9.83	10.29	10.13	11.16	11.11	10.98	11.39	11.37	11.48
H_2O^b	3.44	3.41	3.56	3.50	4.43	4.41	4.45	4.46	4.43	4.22
F	0.63	0.65	0.56	0.68	n.d.	n.d.	n.d.	n.d.	n.d.	0.42
Cl	0.20	0.23	n.d.	0.07	n.d.	0.04	n.d.	n.d.	n.d.	n.d.
O=F	−0.27	−0.27	−0.24	−0.29	n.d.	n.d.	n.d.	n.d.	n.d.	−0.18
O=Cl	−0.04	−0.05	n.d.	−0.01	n.d.	−0.01	n.d.	n.d.	n.d.	n.d.
$\sum$	99.50	99.14	99.55	99.41	99.63	100.32	100.28	100.33	100.08	99.80
Si	6.18	6.09	6.06	6.03	6.66	6.61	6.52	6.51	6.60	6.56
$Al^{(IV)}$	1.83	1.91	1.94	1.97	1.34	1.39	1.48	1.49	1.40	1.44
$Al^{(VI)}$	0.71	0.61	0.95	0.72	2.71	2.95	2.99	2.96	3.25	3.22
Ti	0.68	0.74	0.65	0.64	0.30	0.01	0.27	0.20	0.03	0.04
Cr	n.d.	n.d.	0.01	0.01	0.01	n.d.	0.01	0.01	n.d.	n.d.
Fe^{3+}	n.d.	n.d.	n.d.	n.d.	0.02	0.33	n.d.	0.15	0.09	0.14
Fe^{2+}	2.28	2.35	2.00	2.03	0.29	0.05	0.25	0.10	0.44	0.42
Mn	0.01	0.01	<0.01	0.01	n.d.	0.01	n.d.	<0.01	0.01	0.02
Mg	2.33	2.29	2.49	2.59	0.67	0.66	0.48	0.58	0.19	0.16
Ba	0.02	0.02	0.02	0.01	0.02	0.07	0.02	0.01	<0.01	<0.01
Ca	n.d.	n.d.	n.d.	n.d.	<0.01	n.d.	0.02	n.d.	n.d.	n.d.
Na	0.01	0.01	n.d.	<0.01	0.02	0.03	0.02	0.02	0.05	0.02
K	2.01	2.00	2.06	2.03	1.93	1.92	1.88	1.94	1.96	1.99
O^b	1.15	1.11	1.16	1.04	n.d.	n.d.	n.d.	n.d.	n.d.	n.d.
OH	3.63	3.61	3.72	3.64	3.99	3.99	3.99	3.99	4.00	3.82
F	0.32	0.33	0.28	0.34	n.d.	n.d.	n.d.	n.d.	n.d.	0.18
Cl	0.05	0.06	n.d.	0.02	0.01	0.01	0.01	<0.01	n.d.	n.d.

[a] Formulae normalized to 12 small cations for phengitic white micas and 14 small cations for biotites; [b] calculated; n.d., not detected. Biotite analyses from undeformed metagranitoids from Monte Mucrone [nos. 1 and 2] and from relict metapelites from Val Savenca [nos. 3 and 4]. White micas from Monte Mucrone, replacing Ti-rich biotite [no. 5] and K-feldspar [no. 6]. White micas from Val Savenca, replacing former biotites [nos. 7 and 8] and matrix muscovites from Montestrutto [no. 9] and Tavagnasco [no. 10].

Table 6. Representative electron microprobe analyses of zoisite and titanite[a].

	1	2	3	4	5	6	7	8
SiO_2	38.99	39.28	39.45	39.83	40.36	38.89	30.86	31.06
TiO_2	n.d.	n.d.	0.01	0.02	n.d.	n.d.	36.69	33.76
Al_2O_3	33.78	33.71	33.31	32.44	32.51	31.65	2.55	4.21
Cr_2O_3	n.d.	0.02	0.02	0.03	n.d.	0.05	n.d.	0.06
Fe_2O_3	0.21	0.14	0.47	1.46	1.56	3.43	0.18	0.20
La_2O_3	n.d.	0.02	0.04	n.d.	0.06	n.d.	n.d.	n.d.
Ce_2O_3	0.05	0.03	n.d.	n.d.	0.05	0.09	0.08	0.12
Nd_2O_3	0.02	0.05	0.10	n.d.	n.d.	n.d.	n.d.	0.24
Nb_2O_5	n.a.	n.a.	n.a.	n.a.	n.a.	n.a.	0.04	0.11
Ta_2O_5	n.a.	n.a.	n.a.	n.a.	n.a.	n.a.	0.12	n.d.
MnO	0.04	0.01	n.d.	0.04	n.d.	n.d.	0.03	0.03
CaO	24.20	24.76	24.44	23.98	24.03	24.06	28.56	28.80
SrO	0.14	n.d.	n.d.	0.08	n.d.	n.d.	n.d.	n.d.
F	n.d.	n.d.	n.d.	n.d.	n.d.	n.d.	0.48	1.14
H_2O[b]	1.97	1.98	1.97	1.97	1.99	1.96	0.12	0.12
O=F	n.d.	n.d.	n.d.	n.d.	n.d.	n.d.	−0.20	−0.48
∑	99.39	99.99	99.81	99.85	100.56	100.13	99.50	99.38
Si	2.97	2.99	3.01	3.04	3.08	2.96	1.00	1.00
Al	3.03	3.03	2.99	2.91	2.92	2.84	0.10	0.16
Ti	n.d.	n.d.	0.01	<0.01	n.d.	n.d.	0.89	0.82
Cr	n.d.	<0.01	<0.01	<0.01	n.d.	<0.01	n.d.	<0.01
Fe^{3+}	0.01	0.01	0.03	0.08	0.09	0.20	0.01	<0.01
La	n.d.	0.001	0.01	n.d.	<0.01	n.d.	n.d.	n.d.
Ce	<0.01	<0.01	n.d.	n.d.	<0.01	<0.01	<0.01	<0.01
Nd	<0.01	<0.01	<0.01	n.d.	n.d.	n.d.	n.d.	<0.01
Nb	n.a.	n.a.	n.a.	n.a.	n.a.	n.a.	<0.01	<0.01
Ta	n.a.	n.a.	n.a.	n.a.	n.a.	n.a.	<0.01	n.d.
Mn	<0.01	<0.01	n.d.	<0.01	n.d.	n.d.	<0.01	<0.01
Sr	0.01	n.d.	n.d.	<0.01	n.d.	n.d.	n.d.	n.d.
Ca	1.98	2.02	2.00	1.96	1.96	1.97	0.99	0.99
F	n.d.	n.d.	n.d.	n.d.	n.d.	n.d.	0.05	0.12
OH[b]	1.00	1.01	1.00	1.00	1.01	1.00	0.05	0.05

[a] Formulae normalized to 12.5 oxygens for zoisite and 1 Si cation for titanite; [b] calculated; n.d., not detected; n.a., not analysed. Zoisite analyses from plagioclase pseudomorphs from Monte Mucrone sample MC 1 [nos. 1, 2 and 3] and from Val Savenca samples VS 8 [nos. 4 and 5] and VS 27 [no. 6]. Titanite analyses from phengite–titanite pseudomorphs after biotite [nos. 7 and 8] in Val Savenca sample VS 31.

Table 7. Margules parameters for feldspar and pyroxene solid solutions[a].

	W_E	W_S	W_V (10^3)	Reference
Albite–microcline				
$W_{G,Ab}$	33.363	0.027	0.460	Bachinski & Müller (1971)
$W_{G,Ksp}$	31.345	0.009	0.460	
Analbite–sanidine				
$W_{G,Ab}$	19.541	0.011	0.326	Model 1; Hovis *et al.* (1991)
$W_{G,Ksp}$	22.805	0.007	0.460	
$W_{G,Ab}$	20.079	0.011	0.326	Model 2; Hovis *et al.* (1991)
$W_{G,Ksp}$	20.079	0.002	0.460	
Jadeite–diopside				
$W_{G,Jd-Di}$	26.000			Holland (1990)
Jadeite–hedenbergite				
$W_{G,Jd-Hd}$	25.000			

[a] Units in kJ/mol; $W_H = W_E + PW_V$; $W_G = W_H - TW_S$; $W_G = W_E - TW_S + PW_V$.

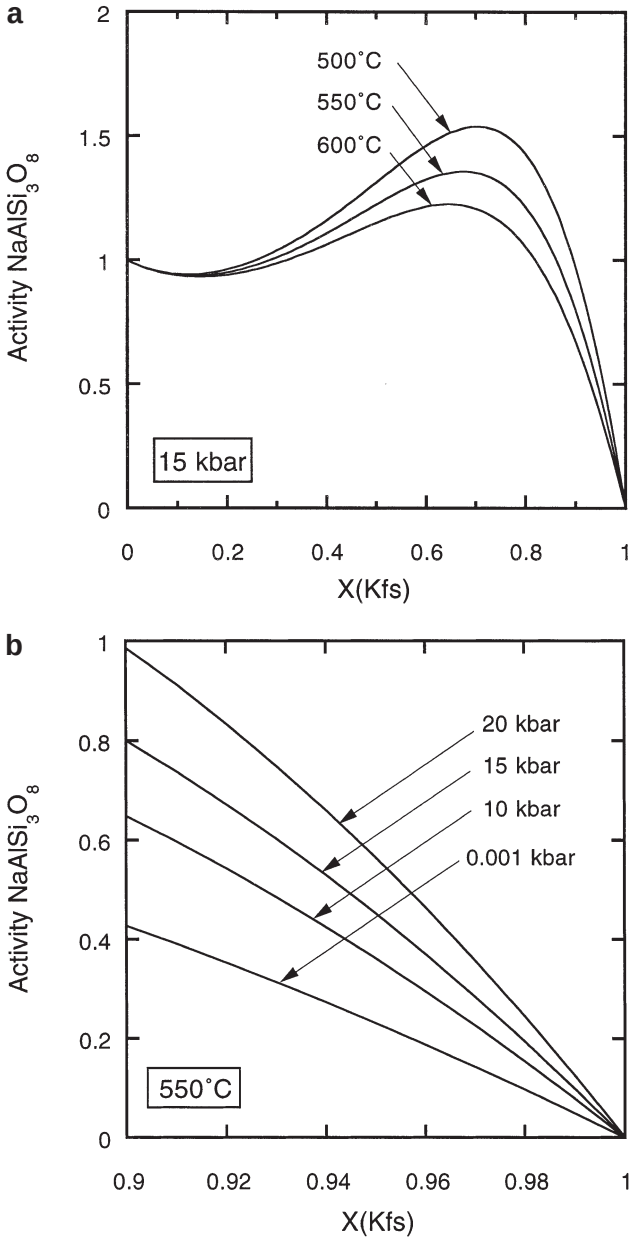

Fig. 5. Activity–composition diagram for disordered alkali feldspar, calculated with the Margules parameters of Hovis *et al.* (1991): (a) temperature dependency of the solvus at 15 kbar; (b) pressure dependency of the Na-poor limb of the solvus in the range 0–10 mol% $NaAlSi_3O_8$ at 550 °C.

omphacite forms over a narrow temperature range in the vicinity of 850 °C (Carpenter, 1981) rather than continuously and linearly over the entire temperature range for which the model was fit (Ganguly & Saxena, 1987).

The equilibrium constant K for reaction (1) was contoured in P–T space by using the experimental reversal brackets of Newton & Smith (1967) at 500 °C, Holland (1980) at 800 °C and of Liu & Bohlen (1995) at 600 °C, 700 °C and 900 °C. The ln K lines in Fig. 7 were computed with available volume, compressibility and expansivity data (Table 8) and calculated $a(NaAlSi_3O_8)$ and $a(NaAlSi_2O_6)$ from Appendix 1, using the relations:

$$\int \Delta V \mathrm{d}P = -\mathrm{R}T \ln K \quad (7)$$

$$\Delta P = -\mathrm{R}T \ln K/\Delta V \quad (8)$$

$$K = a_{(NaAlSi_3O_8)}/a_{(NaAlSi_2O_6)} \quad (9)$$

where ΔP is the pressure shift from the equilibrium curve for $K=1$, K is the equilibrium constant for

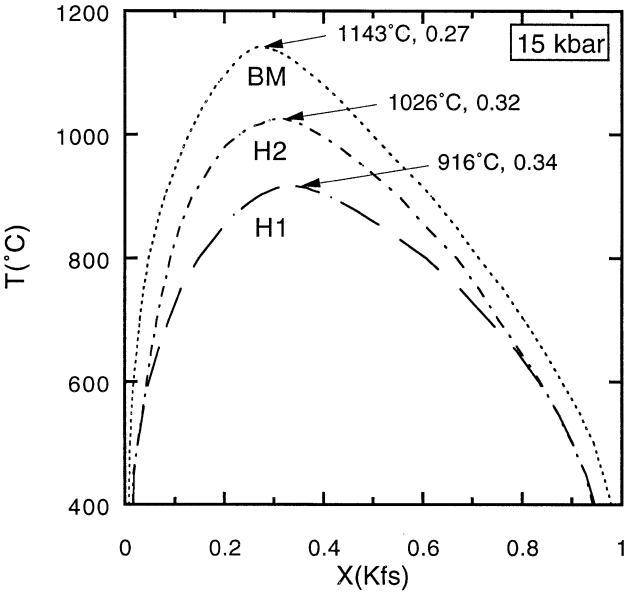

Fig. 6. Low albite–low microcline and analbite–sanidine solvi, calculated at 15 kbar. The solvus of the ordered triclinic modifications was calculated with the Margules parameters of Bachinski & Müller (1971) (BM, dotted line). Two different solvi of the disordered monoclinic modifications were calculated with the Margules parameters of Hovis *et al.* (1991): model H1 (dashed line); model H2 (dashed/dotted line). The critical temperatures and K-feldspar compositions, X(Kfs) are also given.

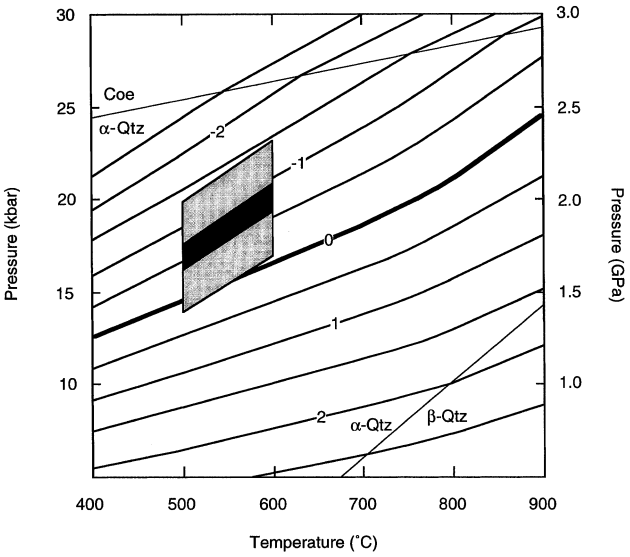

Fig. 7. *P–T* diagram with lines of constant ln K and the results of the calculations for samples from Monte Mucrone, Montestrutto, Tavagnasco and Val Savenca. The dark field indicates the pressure range calculated with the disordered model and the grey fields represent 2σ errors. Also shown are the quartz–coesite transition (Bohlen & Boettcher, 1982) and α-β quartz transition (Cohen & Klement, 1967).

reaction (1), R is the universal gas constant (8.3144 J/mol K) and ΔV is the volume change at equilibrium. The curvature in the ln K lines between 680 and 790 °C is due to the structural transition from low to high albite (Goldsmith & Jenkins, 1985). The difference in pressure using compressibilities and expansivities from different databases (Berman, 1988; Saxena *et al.*, 1993) is small and generates less than a 0.2 kbar shift in the ln K curves.

Because of the spread in temperature estimates which were available in the literature, pressures were calculated at 500, 550 and 600 °C for all samples. Since the estimated temperatures are well below the low albite/high albite transition temperature, only low albite was used in the calculations. For typical metagranite and metapelite assemblages of K-feldspar (Ab_{4-11})–jadeite (Jd_{80-97})–quartz (KJQ), reaction (1) is shifted 1–4 kbar higher than the end-member reaction at 550 °C by using the disordered activity model for K-feldspar of Hovis *et al.* (1991) (Fig. 7; Appendix 2). For comparison, pressures obtained with the activity model for ordered K-feldspar of Bachinski & Müller (1971), yield pressures that are 0.2–2.5 kbar higher than the end-member reaction. The pressures have been obtained through iteration by calculating the alkali feldspar activity at pressures of 15, 17 and 19 kbar. This iteration was performed until the pressure values of each sample converged to <0.1 kbar. The error estimation for these calculations includes errors propagated from analytical uncertainties, based on counting statistics on the microprobe ($\Delta X_{Ab}=0.006$) which results in an error of 0.4 kbar, uncertainties in the experimental brackets of reaction (1) (0.1 kbar precision; 0.2–0.4 kbar width of bracket) and estimated errors in the W_G parameters of the activity model of Hovis *et al.* (1991) (± 2.5 kJ/mol in $W_{G,Ab}$). The uncertainty in W_G leads to a 2σ uncertainty in the activity of $NaAlSi_3O_8$ in sanidine of 0.6 ± 0.25 which corresponds to a 2σ error estimate of 1.5–1.8 kbar. No error estimation for the microcline activity model of Bachinski & Müller (1971) was possible, since the authors did not report the uncertainties in their model. In contrast, the errors based on the activity model for pyroxene by Holland (1990) are very small. Error propagation of the uncertainties in W_A and W_B in the activity model for the activity of $NaAlSi_2O_6$ yields 2σ errors of 0.0005–0.007 because the composition of jadeite is very close to end-member composition. When analytical, experimental and thermodynamic errors are combined as independent values, an overall error of 1.6–1.9 kbar is obtained for the disordered modifications (shown as grey area in Fig. 7). Besides the errors discussed above, the compositional variation of K-feldspar grains within one sample or between several samples also needs to be taken into account. These variations in X(Kfs) result in a pressure range rather than one pressure for a given temperature. This is indicated in the black field in Fig. 7, which includes the pressure variation within a sample and between the samples from the four localities. Both are very similar to each other and result in pressure variations of 1.2 and 1.4 kbar for a given temperature.

Table 8. Volume, compressibility and expansivity data used in thermodynamic calculations.

Phase	[a]V°_{298}	Ref.	a	b (10^{-3})	c (10^{-6})	d (10^{-10})	Ref.	e (10^{-6})	f (10^{-12})	Ref.
Albite (low)	9.998	(5)	−0.433	0.873	2.091	−4.958	(5)	1.807	7.851	(5)
Albite (high)	10.045	(2)	−1.017	4.079	−2.643	14.100	(1)	1.807	7.851	(5)
Jadeite	6.040	(11)	−0.246	−0.092	3.529	−14.576	(3)	0.822	1.584	(6)
α-Quartz	2.269	(11)	−0.698	1.882	2.280	7.033	(4)	2.677	18.127	(7)
β-Quartz	2.379	(8)	0.129	−0.374	−0.175	0.576	(8)	1.780	0.000	(9)
Coesite	2.064	(11)	−0.169	0.401	0.569	−0.559	(10)	1.218	6.046	(7)

[a] V°_{298} (J/bar); $V_{P,298}=V^{\circ}_{298}(1-aP+bP^2)$, P in bar; $V_{T,1\ bar}=V^{\circ}_{298}+V_{298}/100[c+dT+eT^2+fT^3]$, T in K.
References: (1) Winter *et al.* (1977); (2) Winter *et al.* (1979); (3) Cameron *et al.* (1973); (4) Moecher *et al.* (1988); (5) Downs *et al.* (1994); (6) McCormick *et al.* (1989); (7) Jorgensen (1978); (8) Moecher & Essene (1990); (9) Levien & Prewitt (1981); Birch (1966); (11) Robie & Hemingway (1995).

DISCUSSION

The KJQ barometry may be compared with other thermobarometers that apply to these metagranites. The presence of jadeite in the pyroxene (Jd_{80-96}) indicates a minimum pressure of 14–16 kbar in the presence of quartz without albite, and the absence of coesite limits the rocks to <25–27 kbar at temperatures of 500–600 °C (Bohlen & Boettcher, 1982). The upper stability of K-feldspar at crustal temperatures is at 25 kbar (Thompson *et al.*, 1998; Fasshauer *et al.*, 1997) before it reacts with H_2O to form a K-feldspar hydrate.

The application of KJQ barometry yields a direct determination of pressure in high-pressure quartzo-feldspathic rocks. Although Compagnoni & Maffeo (1973) and Biino & Compagnoni (1992) regarded K-feldspar in eclogitic metagranites as a metastable relict, the textures in the rocks from this study suggest that a new K-feldspar equilibrated with the high-pressure assemblage jadeite–kyanite–zoisite–quartz. The total pressure range using the disordered model for K-feldspar ranges from 15 to 21 kbar in the temperature region of interest (Appendix 2). These calculated pressures are somewhat higher than the range of pressure estimates obtained from the Sesia-Lanzo Zone by previous workers (Fig. 8). Most previous estimates in the range of 14–17 kbar are based on the limiting assemblage jadeite–quartz, although Pognante (1989) used the paragonite breakdown reaction (4) to derive an upper pressure limit of 20 kbar from the absence of kyanite, assuming the presence of pure H_2O fluid with $P_{H_2O}=P_T$. Since omphacite grows in the partially re-equilibrated samples of Monte Mucrone and Val Savenca, sometimes at the rims of jadeite but without albite, it is also possible to infer minimum pressures of 12–14 kbar for temperatures between 500 and 600 °C.

The direct determination of pressures in eclogites in combination with temperature estimates make it possible to constrain $a_{(H_2O)}$ for the partially equilibrated samples from Val Savenca with the assemblage jadeite–kyanite. The $a_{(H_2O)}$ has been evaluated by contouring a P–T diagram with $a_{(H_2O)}$-isopleths for reaction (4) with the database of Holland & Powell (1990) and an updated version of THERMOCALC version 2.3 (Holland, written communication, 1994). Since paragonite is absent, this provides a lower limit for $a_{(H_2O)}$ in the P–T space (Fig. 8). Propagating the errors in this calculation, the obtained $a_{(H_2O)}$ is 0.2– 0.6 for the partially re-equilibrated samples from Val Savenca. The assemblage jadeite–kyanite has been described only from a few locations in the Western Alps (Dora Maira: Chopin, 1984; Allalin metagabbro: Wayte *et al.*, 1989). The whiteschists from Dora Maira were metamorphosed at 700–800 °C and 34–37 kbar (Schertl *et al.*, 1991; Sharp *et al.*, 1993). Chopin (1984) suggested an $a_{(H_2O)}$ of 0.2 for the ultra-high-pressure rocks from Dora Maira, due to the absence of melting, and later he and Schertl *et al.* (1991) proposed $a_{(H_2O)}=1$, based on available phase equilibria. Sharp *et al.* (1993)

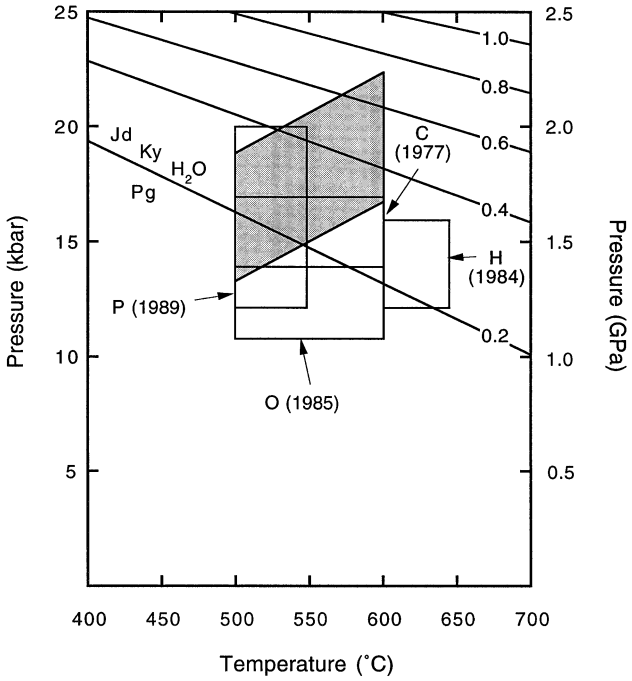

Fig. 8. Comparison of the pressure estimates from this study obtained with the disordered K-feldspar activity model with literature estimates for the Sesia-Lanzo Zone—C: Compagnoni *et al.* (1977); O: Oberhänsli *et al.* (1985); P: Pognante (1989); H: Hy (1984)—and estimation of $a_{(H_2O)}$ limits for the assemblage jadeite–kyanite from the partially re-equilibrated metapelites from Val Savenca. The estimation of $a_{(H_2O)}$ is based on the reaction paragonite (Pg)=jadeite (Jd)+kyanite (Ky)+H_2O and the numbers on the right-hand side of the diagram represent values of constant $a_{(H_2O)}$ along each curve.

obtained an $a_{(H_2O)}$ of 0.4–0.7 for these rocks based on an independent temperature estimate, by using stable isotope thermometry. The Allalin metagabbro has been subjected to metamorphic conditions of 600 °C and 20 kbar (Meyer, 1983), which would indicate a low $a_{(H_2O)}$ of 0.5. Wayte *et al.* (1989) concluded that fluid absence would account for the failure of completion of the plagioclase breakdown reaction in the plagioclase domains and concentration gradients in the relict plagioclase.

Application of mixing models in the system $NaAlSi_3O_8$-$KAlSi_3O_8$ still presents several problems. Firstly, the uncertainty in the thermodynamic data leads to large errors. Hovis *et al.* (1991) pointed out that small uncertainties in the solvus brackets for the system analbite–sanidine result in large errors for the derived thermodynamic data. Secondly, Powell (1974) showed that the Ab–Or solvus could be fitted satisfactorily by several different models (Van Laar, subregular, asymmetric quasichemical model). These models reproduce the solvus but give different results for pressures when applied to the Ab = Jd + Qtz barometer. Thus the choice of the model affects the results. Finally, the analytical uncertainty becomes important because the molar proportion of albite in the K-feldspar is very small, 0.05–0.1. Despite the uncertainties, KJQ barometry is nonetheless useful for eclogite facies rocks where pressures are seldom otherwise well fixed. This in turn allows a better estimation of $a_{(H_2O)}$ that otherwise is ill-constrained in most eclogitic rocks.

ACKNOWLEDGEMENTS

This work was supported by NSF grants EAR 95-26596 and 92-05649 from the National Science Foundation to E.J.E., and a fellowship from the Austrian Bundesministerium für Wissenschaft und Forschung and grants from the International Institute of the University of Michigan, Turner Fund of the Department of Geological Sciences at the University of Michigan, and the Geological Society of America to P.T. The senior author thanks G. Venturini for his help in the field in Val Savenca, Montestrutto and Tavagnasco and Prof. G. Hoinkes for providing some of the samples from Monte Mucrone. Dr G. Martinotti is also thanked for providing samples at the early stage of this work. Li-Shun Kao and G. Simon are thanked for help with the X-ray diffractometer, L. Wang for his help with error propagations and C. Henderson for valuable help on the electron microprobe. Reviews by B. Evans, G. Franz and two anonymous reviewers and the editorial handling by M. Brown are gratefully acknowledged and helped to clarify the manuscript considerably. The electron microprobe used in this study was purchased by NSF grant EAR 82-12764 from the National Science Foundation and the scanning electron microscope by NSF grant BSR 83-14092.

REFERENCES

Afifi, A. & Essene, E. J., 1988. MINFILE, a microcomputer program for storage and manipulation of chemical data on minerals. *American Mineralogist*, **73,** 446–448.

Ahn, J. H., Essene, E. J. & Peacor, D. R., 1985. Coexisting paragonite–phengite in blueschist eclogite: a TEM study. *American Mineralogist*, **70,** 1193–1204.

Ai, Y., 1994. A revision of the garnet–clinopyroxene Fe^{2+}–Mg exchange geothermometer. *Contributions to Mineralogy and Petrology*, **115,** 465–473.

Andersen, T., Burke, E. A. J. & Austrheim, H., 1989. Nitrogen-bearing, aqueous fluid inclusions in some eclogites from the Western Gneiss region of the Norwegian Caledonides. *Contributions to Mineralogy and Petrology*, **103,** 153–165.

Andersen, T., Austrheim, H., Burke, E. A. J. & Elvevold, S., 1993. N_2 and CO_2 in deep crustal fluids; evidence from the Caledonides of Norway. *Chemical Geology*, **108,** 113–132.

Bachinski, S. W. & Müller, G., 1971. Experimental determinations of the microcline–low albite solvus. *Journal of Petrology*, **12,** 329–356.

Barbero, M., 1992. *Geologia dell'alto vallone del Savenca (Zona Sesia-Lanzo, Alpi Occidentali). Msc Thesis, University of Torino, Torino, Italy.*

Barnicoat, A. C. & Fry, N., 1986. High-pressure metamorphism of the Zermatt-Saas ophiolite Zone, Switzerland. *Journal of the Geological Society of London*, **143,** 607–618.

Barnicoat, A. C. & Fry, N., 1989. Eo-Alpine high-pressure metamorphism in the Piemonte Zone of the Alps, south-west Switzerland and northwest Italy. In: *Evolution of Metamorphic Belts* (eds Daly, J. S., Cliff, R. A. & Yardley, B. W. D.), *Geological Society of London Special Publication*, **44,** 539–544.

Berman, R. G., 1988. Internally-consistent thermodynamic data for minerals in the system Na_2O–K_2O–CaO–FeO–Fe_2O_3–Al_2O_3–SiO_2–TiO_2–H_2O–CO_2. *Journal of Petrology*, **29,** 445–522.

Bernotat, W. H. & Bambauer, H. U., 1982. The microcline/sanidine transformation isograd in metamorphic regions: II. The region of Lepontine metamorphism, Central Swiss Alps. *Schweizerische Mineralogische und Petrographische Mitteilungen*, **62,** 231–244.

Biino, G. G. & Compagnoni, R., 1992. Very high pressure metamorphism of the Brossasco coronite metagranite, southern Dora Maira Massif, Western Alps. *Schweizerische Mineralogische und Petrologische Mitteilungen*, **72,** 347–363.

Birch, F., 1966. Compressibility: elastic constraints. In: *Handbook of Physical Constants* (ed Clark, S. P. Jr), *Geological Society of America Memoir*, **93,** 97–173.

Bohlen, S. R. & Boettcher, A. L., 1982. The quartz–coesite transformation: a precise determination and the effects of other components. *Journal of Geophysical Research*, **87,** 7073–7078.

Bohlen, S. R., Peacor, D. R. & Essene, E. J., 1980. Crystal chemistry of a metamorphic biotite and its significance in water barometry. *American Mineralogist*, **65,** 55–62.

Brown, W. L. & Parsons, I., 1989. Alkali feldspars; ordering rates, phase transformations and behavior diagrams for igneous rocks. *Mineralogical Magazine*, **53,** 25–42.

Cameron, M., Sueno, S., Prewitt, C. T. & Papike, J. J., 1973. High temperature crystal chemistry of acmite, diopside, hedenbergite, jadeite, spodumene and ureyite. *American Mineralogist*, **58,** 594–618.

Carpenter, M. A., 1981. Omphacite microstructures as time–temperature indicators of blueschist- and eclogite-facies metamorphism. *Contributions to Mineralogy and Petrology*, **78,** 441–451.

Carpenter, M. A. & Putnis, A., 1986. Cation order and disorder during crystal growth: some implications for natural mineral assemblages. In: *Metamorphic Reactions. Kinetics, Textures and Deformation* (eds Thompson, A. B. & Rubie, D. C.), pp. 1–26. Springer Verlag, New York.

Carpenter, M. A. & Salje, E. K. H., 1994. Thermodynamics of

non-convergent cation ordering in minerals: III. Order parameter coupling in potassium feldspar. *American Mineralogist*, **79,** 1084–1098.

Chopin, C., 1984. Coesite and pure pyrope in high-grade blueschists of the western Alps: a first record and some consequences. *Contributions to Mineralogy and Petrology*, **86,** 107–118.

Cohen, L. H. & Klement, W., 1967. High–low quartz inversion: determination to 35 kilobars. *Journal of Geophysical Research*, **72,** 4245–4251.

Compagnoni, R. & Maffeo, B., 1973. Jadeite-bearing metagranites l.s. & related rocks in Monte Mucrone area (Sesia-Lanzo Zone, Western Italian Alps). *Schweizerische Mineralogische und Petrographische Mitteilungen*, **53,** 355–378.

Compagnoni, R., Dal Piaz, G. V., Hunziker, J. C., Gosso, G., Lombardo, B. & Williams, P. F., 1977. The Sesia-Lanzo Zone, a slice of continental crust with Alpine high pressure–low temperature assemblages in the western Italian Alps. *Rendiconti Della Societa Italiana di Mineralogia e Petrologia*, **33,** 281–334.

Compagnoni, R., Hirajima, T. & Chopin, C., 1995. Ultra high pressure metamorphic rocks in the Western Alps. In: *Ultrahigh Pressure Metamorphism* (eds Coleman, R. G. & Wang, X.), pp. 206–244. Cambridge University Press, New York.

Dal Piaz, G. V., Hunziker, J. C. & Martinotti, G., 1972. La Zona Sesia-Lanzo e l'evoluzione tectonico-metamorphica della Alpi nordoccidentali interne. *Memorie della Societa Geologica Italiana*, **11,** 433–466.

Downs, R. T., Hazen, R. M. & Finger, L. W., 1994. The high pressure crystal chemistry of low albite and the origin of the pressure dependency of Al–Si ordering. *American Mineralogist*, **79,** 1042–1052.

Droop, G. T. R., Lombardo, B. & Pognante, U., 1990. Formation and distribution of eclogite facies rocks in the Alps. In: *Eclogite Facies Rocks* (ed Carswell, D. A.), pp. 225–259. Blackie, Glasgow.

Ellis, D. J. & Green, D. H., 1979. An experimental study on the effect of Ca upon garnet–clinopyroxene exchange equilibria. *Contributions to Mineralogy and Petrology*, **71,** 12–22.

Essene, E. J., 1982. Geologic thermometry and barometry. In: *Characterization of Metamorphism through Mineral Equilibria* (ed Ferry, J. M.), *Mineralogical Society of America, Reviews in Mineralogy*, **10,** 153–206.

Essene, E. J., 1989. The current status of thermobarometry in metamorphic rocks. In: *Evolution of Metamorphic Belts* (eds Daly, J. S., Cliff, R. A. & Yardley, B. W. D.), *Geological Society of London Special Publication*, **43,** 1–44.

Essene, E. J. & Fyfe, W. S., 1967. Omphacite in Californian metamorphic rocks. *Contributions to Mineralogy and Petrology*, **15,** 1–23.

Essene, E. J., Hensen, B. J. & Green, D. H., 1970. Experimental study of amphibolite and eclogite stability. *Physics of Earth and Planetary Interiors*, **3,** 378–384.

Evans, B., 1990. Phase relations of epidote-blueschists. *Lithos*, **25,** 3–25.

Fasshauer, D. W., Chatterjee, N. D. & Marler, B., 1997. Synthesis, structure, thermodynamic properties, and stability relations of K-cymrite, $K[AlSi_3O_8]\cdot H_2O$. *Physics and Chemistry of Minerals*, **24,** 455–462.

Früh-Green, G. L., 1987. *Stable isotope investigations of fluid–rock interaction during metamorphism and exhumation of eclogite-facies rocks: case studies from the Swiss and Italian Alps.* PhD Thesis, Eidgenössische Technische Hochschule, Zürich.

Fry, N. & Fyfe, W. S., 1969. Eclogites and water pressure. *Contributions to Mineralogy and Petrology*, **24,** 1–6.

Fry, N. & Fyfe, W. S., 1971. On the significance of the eclogite facies in Alpine metamorphism. *Verhandlungen der Geologischen Bundesanstalt*, **2,** 257–265.

Ganguly, J. & Saxena, S. K., 1987. *Mixtures and mineral reactions.* Springer Verlag, New York.

Ganguly, J., Weiji, C. & Tirone, M., 1996. Thermodynamics of aluminosilicate garnet solid solution: new experimental data, an optimized model and thermometric applications. *Contributions to Mineralogy and Petrology*, **126,** 137–151.

Gasparik, T., 1985. Experimentally determined compositions of diopside–jadeite pyroxene in equilibrium with albite and quartz at 1200–1350 °C and 15–34 kb. *Geochimia Cosmochimia Acta*, **49,** 65–87.

Goldsmith, J. R. & Jenkins, D. M., 1985. The high–low albite relations revealed by reversal of degree of order at high pressure. *American Mineralogist*, **70,** 911–923.

Green, T. H. & Adam, J., 1991. Assessment of the garnet–clinopyroxene Fe–Mg exchange thermometer using new experimental data. *Journal of Metamorphic Geology*, **9,** 341–348.

Holland, T. J. B., 1979a. Experimental determination of the reaction paragonite = jadeite + kyanite + H_2O and thermodynamic data for part of the system Na_2O–Al_2O_3–SiO_2–H_2O, with applications to eclogites and blueschists. *Contributions to Mineralogy and Petrology*, **68,** 293–301.

Holland, T. J. B., 1979b. High water activities in the generation of high-pressure kyanite eclogites of the Tauern Window, Austria. *Journal of Geology*, **7,** 1–27.

Holland, T. J. B., 1980. The reaction albite = jadeite + quartz determined experimentally in the range 600–1200 °C. *American Mineralogist*, **65,** 129–134.

Holland, T. J. B., 1983. The experimental determination in disordered and short-range ordered jadeitic pyroxenes. *Contributions to Mineralogy and Petrology*, **82,** 214–220.

Holland, T. J. B., 1990. Activities of components in omphacitic solid solutions. An application of Landau theory to mixtures. *Contributions to Mineralogy and Petrology*, **105,** 446–453.

Holland, T. J. B. & Powell, R., 1990. An enlarged and updated internally consistent thermodynamic data set with uncertainties and correlations: the system K_2O–Na_2O–CaO–MgO–MnO–FeO–Fe_2O_3–Al_2O_3–TiO_2–SiO_2–C–H_2–O_2. *Journal of Metamorphic Geology*, **8,** 89–124.

Hovis, G. L., 1986. Behavior of alkali feldspars: crystallographic properties and characterization of composition and Al–Si distribution. *American Mineralogist*, **71,** 869–890.

Hovis, G. L., 1988. Enthalpies and volumes related to K–Na mixing and Al–Si order/disorder in alkali feldspars. *Journal of Petrology*, **29,** 731–763.

Hovis, G. L., Delbove, F. & Roll-Bose, M., 1991. Gibbs energies and entropies of K–Na mixing for alkali feldspars from phase equilibrium data: implications for feldspar solvi and short-range order. *American Mineralogist*, **76,** 913–927.

Hy, C., 1984. *Metamorphisme polyphase et evolution tectonique dans la croute continentale eclogitisee: les series granitiques et pelitiques du Monte Mucrone (Zone Sesia-Lanzo, Alpes Italiennes).* Thése 3é Cycle, Université de Paris, Paris VI.

Jamtveit, B., Bucher-Nurminen, K. & Austrheim, H., 1990. Fluid controlled eclogitization of granulites in deep crustal shear zones, Bergen Arcs, Norway. *Contributions to Mineralogy and Petrology*, **104,** 184–193.

Jorgensen, J. D., 1978. Compression mechanisms in α-quartz structures SiO_2 and GeO_2. *Journal of Applied Physics*, **49,** 5473–5478.

Kennedy, C. S. & Kennedy, G. C., 1976. The equilibrium boundary between graphite and diamond. *Journal of Geophysical Research*, **81,** 2467–2470.

Klemd, R., 1989. *P–T* evolution and fluid inclusion characteristics of retrograded eclogites, Münchberg Gneiss Complex, Germany. *Contributions to Mineralogy and Petrology*, **102,** 221–229.

Koons, P. O., 1984. Implications to garnet–clinopyroxene geothermometry of non-ideal solid solution in jadeitic pyroxenes. *Contributions to Mineralogy and Petrology*, **88,** 340–347.

Koons, P. O., 1986. Relative geobarometry from high-pressure rocks of quartzofeldspatic composition from the Sesia Zone, Western Alps, Italy. *Contributions to Mineralogy and Petrology*, **93,** 322–334.

Koons, P. O., Rubie, D. C. & Früh-Green, G. L., 1987. The effects of dis-equilibrium and deformation on the mineralogical evolution of quartz diorite during metamorphism in the eclogite facies. *Journal of Petrology*, **28,** 679–700.

Kretz, R., 1983. Symbols for rock-forming minerals. *American Mineralogist*, **68,** 277–279.

Krogh, E. J., 1988. The garnet–clinopyroxene Fe–Mg geothermometer—a reinterpretation of existing experimental data. *Contributions to Mineralogy and Petrology*, **99,** 44–48.

Kroll, H. & Ribbe, P. H., 1983. Lattice parameters, composition and Al,Si order in alkali feldspars. In: *Feldspar Mineralogy* (ed. Ribbe, P. H.), *Mineralogical Society of America, Reviews in Mineralogy*, **2,** 58–98.

Kroll, H., Krause, C. & Voll, G., 1991. Disordering, re-ordering and unmixing in alkali-feldspars from contact metamorphosed quartzites. In: *Equilibrium and Kinetics in Contact Metamorphism: the Ballachulish Igneous Complex and its Aureole* (eds Voll, G., Töpel, J., Pattison, D. R. M. & Seifert, F.), pp. 267–296. Springer Verlag, Heidelberg.

Lefévre, R. & Michard, A., 1965. La jadeite dans le metamorphisme alpin, a propos des gisements de type noveau, de la bande d'Acceglio (Alpes cottiénnes, Italie). *Bulletin de la Societe Francaise de Minéralogie et de Cristallographie*, **88,** 664–677.

Le Goff, E. & Ballevre, M., 1990. Geothermobarometry in albite–garnet orthogneisses: a case study from the Gran Paradiso nappe (Western Alps). *Lithos*, **25,** 261–280.

Levien, L. & Prewitt, C. T., 1981. High pressure crystal structure and compressibility of coesite. *American Mineralogist*, **66,** 324–333.

Liu, J. & Bohlen, S. R., 1995. Mixing properties and stability of jadeite–acmite pyroxene in the presence of albite and quartz. *Contributions to Mineralogy and Petrology*, **119,** 433–440.

Liu, J., Bohlen, S. R. & Ernst, W. G., 1996. Stability of hydrous phases in subducting oceanic crust. *Earth and Planetary Science Letters*, **143,** 161–171.

McCormick, T. C., Hazen, R. M. & Angel, R., 1989. Compressibility of omphacite to 60 kbar: role of vacancies. *American Mineralogist*, **74,** 1287–1292.

Manning, C. E. & Bohlen, S. R., 1991. The reaction titanite + kyanite = anorthite + rutile and titanite–rutile barometry in eclogites. *Contributions to Mineralogy and Petrology*, **109,** 1–9.

Massonne, H. J. & Chopin, C., 1989. *P–T* history of Gran Paradiso (Western Alps) metagranites based on phengite barometry. In: *Evolution of Metamorphic Belts* (eds Daly, J. S., Cliff, R. A. & Yardley, B. W. D.), *Geological Society of London Special Publication*, **44,** 545–549.

Massonne, H. J. & Schreyer, W., 1987. Phengite geobarometry based on the limiting assemblage with K-feldspar, phlogopite and quartz. *Contributions to Mineralogy and Petrology*, **96,** 212–224.

Meyer, J., 1983. The development of the high pressure metamorphism in the Allalin metagabbro (Switzerland). *Terra Cognita*, **3,** 187.

Miller, C., 1974. On the metamorphism of the eclogites and the high-grade blueschists from the Penninic Terrane of the Tauern Window, Austria. *Schweizerische Mineralogische und Petrographische Mitteilungen*, **54,** 371–384.

Moecher, D. P. & Essene, E. J., 1990. Phase equilibria for calcic scapolite, and implications of variable Al–Si disorder for *P–T*, *T–X*CO_2, and *a–X* relations. *Journal of Petrology*, **31,** 997–1024.

Moecher, D. P., Essene, E. J. & Anovitz, L. M., 1988. Calculation and application of clinopyroxene–garnet–plagioclase–quartz geobarometers. *Contributions to Mineralogy and Petrology*, **100,** 92–106.

Morten, L., 1993. *Italian Eclogites and Related Rocks*. Academia Nazionale delle Scienze Detta Dei XL, Roma, Italy.

Newton, R. C., 1986. Metamorphic temperatures and pressures of Group B and Group C eclogites. In: *Blueschists and Eclogites* (eds Evans, B. W. & Brown, E. H.), *Geological Society of America Special Publication*, **164,** 17–30.

Newton, R. C. & Kennedy, G. C., 1963. Some equilibrium reactions in the join $CaAl_2Si_2O_8$–H_2O. *Journal of Geophysical Research*, **68,** 2967–2983.

Newton, R. C. & Smith, J. V., 1967. Investigations concerning the breakdown of albite at depth in the earth. *Journal of Geology*, **75,** 268–286.

Oberhänsli, R., Hunziker, J. C., Martinotti, G. & Stern, W. B., 1985. Geochemistry, geochronology and petrology of Monte Mucrone: an example of Eo-Alpine eclogitization of Permian granitoids in the Sesia-Lanzo Zone, Western Alps, Italy. *Chemical Geology*, **52,** 165–184.

Pattison, D. R. M. & Newton, R. C., 1989. Reversed experimental calibration of the garnet–clinopyroxene Fe–Mg exchange thermometer. *Contributions to Mineralogy and Petrology*, **101,** 87–103.

Pognante, U., 1989. Lawsonite, blueschist and eclogite formation in the southern Sesia Zone (Western Alps, Italy). *European Journal of Mineralogy*, **1,** 89–104.

Pognante, U., Talarico, F., Rastelli, N. & Ferrati, N., 1987. High pressure metamorphism in the nappes of the Valle dell'Orco traverse (Western Alps collisional belt). *Journal of Metamorphic Geology*, **5,** 397–414.

Powell, R., 1974. A comparison of some mixing models for crystalline silicate solid solutions. *Contributions to Mineralogy and Petrology*, **46,** 265–274.

Powell, R., 1985. Regression diagnostics and robust regression in geothermometer/geobarometer calibration: the garnet–clinopyroxene thermometer revisited. *Journal of Metamorphic Geology*, **3,** 327–342.

Robie, R. & Hemingway, B., 1995. Thermodynamic properties of minerals and related substances at 298.15 K and 1 bar (10^5 Pascals) pressure and higher temperatures. *US Geological Survey Bulletin*, **2131,** 461.

Saxena, S. K., Chatterjee, N., Fei, Y. & Shen, G., 1993. *Thermodynamic Data on Oxides and Silicates*. Springer Verlag, New York.

Schertl, H. P., Schreyer, W. & Chopin, C., 1991. The pyrope–coesite rocks and their country rocks at Parigi, Dora Maira Massif, Western Alps: detailed petrography, mineral chemistry and *P–T* path. *Contributions to Mineralogy and Petrology*, **108,** 1–21.

Sharp, Z. D., Essene, E. J. & Smyth, J., 1992. Ultra high temperatures from oxygen isotope thermometry of a coesite–sanidine grospydite. *Contributions to Mineralogy and Petrology*, **112,** 358–370.

Sharp, Z. D., Essene, E. J. & Hunziker, J. C., 1993. Stable isotope geochemistry and phase equilibria of coesite-bearing whiteschists, Dora Maira Massif, Western Alps. *Contributions to Mineralogy and Petrology*, **114,** 1–12.

Stewart, D. R. & Wright, T. L., 1974. Al/Si order and symmetry of natural alkali feldspars and relationship of strained parameters to bulk composition cell. *Bulletin de la Societe Francaise de Mineralogie et Cristallographie*, **97,** 356–377.

Thompson, J. B., 1967. Thermodynamic properties of simple solutions. In: *Researches in Geochemistry, Vol. 2* (ed. Abelson, P. H.), pp. 340–361. Wiley, New York.

Thompson, J. B., 1969. Chemical reactions in crystals. *American Mineralogist*, **54,** 341–375.

Thompson, P., Parsons, I., Graham, C. M. & Jackson, B., 1998. The breakdown of potassium feldspar at high water pressures. *Contributions to Mineralogy and Petrology*, **130,** 176–187.

Venturini, G., 1995. Geology, geochemistry and geochronology of the inner central Sesia Zone (Western Alps-Italy). *Mémoires de Géologie (Lausanne)*, **25,** 147.

Venturini, G., Martinotti, G., Armando, G., Barbero, M. & Hunziker, J. C., 1994. The Central Sesia–Lanzo Zone (Western Italian Alps): new field observations and lithostratigraphic subdivisions. *Schweizerische Mineralogische und Petrographische Mitteilungen*, **74,** 111–121.

Wall, V. J. & Essene, E. J., 1972. Subsolidus equilibria in CaO–Al_2O_3–SiO_2–H_2O. *Geological Society of America Abstracts and Program*, **4,** 700.

Wayte, G. J., Worden, R. H., Rubie, D. C. & Droop, G. T. R., 1989. A TEM study of dis-equilibrium plagioclase breakdown at high pressure: the role of infiltrating fluid. *Contributions to Mineralogy and Petrology*, **101,** 426–437.

Winter, J. K., Ghose, S. & Okamura, F. P., 1977. A high

temperature study of thermal expansion and the anisotropy of the sodium atom in low albite. *American Mineralogist*, **62,** 921–936.

Winter, J. K., Okamura, F. P. & Ghose, S., 1979. A high temperature structural study of high albite, monalbite and the analbite–monalbite phase transition. *American Mineralogist*, **94,** 409–423.

Wood, B. J. & Nicholls, J., 1978. The thermodynamic properties of reciprocal solid solutions. *Contributions to Mineralogy and Petrology*, **66,** 389–400.

Received 10 February 1998; revision accepted 30 August 1998.

APPENDIX 1. ACTIVITY MODELS

The activity coefficients of feldspar solid solution (γ) have been calculated with a subregular Margules model (Thompson, 1967):

$$RT \ln_{Ab} = [W_{G,Ab} + 2(W_{G,Ksp} - W_{G,Ab})(X_{Ab})](X_{Ksp})^2$$

$$RT \ln \gamma_{Ksp} = W_{G,Ksp} + 2(W_{G,Ab} - W_{G,Ksp})(X_{Ksp})](X_{Ab})^2$$

$$a_{(NaAlSi_3O_8)} = X_{ab}\ \gamma_{Ab}$$

$$a_{(KAlSi_3O_8)} = X_{Ks}\ \gamma_{Ksp}$$

and $W_{G,Ab}$, $W_{G,Ksp}$ as in Table 7.

The activity of jadeite has been calculated following Holland (1990), who evaluated the activities of clinopyroxenes in the system jadeite–diopside–hedenbergite–acmite by using a two-site simple reciprocal model (Wood & Nicholls, 1978).

$$RT\ln \gamma_{Jd} = X_{Ca,M2}\,[X_{Mg,M1}\ W_{G,Jd-Di} + X_{Fe^{2+},\ M1}\ W_{G,Jd-Hd}]$$

$$a_{(NaAlSi_2O_6)} = (X_{Na,M2}\ X_{Al,M1})\ \gamma_{Jd}$$

with $W_{G,Jd-Di}$, $W_{G,Jd-Hd}$ as in Table 7 and cation distribution in clinopyroxenes: M2: Na, Ca; M1: Fe^{2+}, Fe^{3+}, Mg.

APPENDIX 2. INPUT DATA AND RESULTS OF BAROMETRIC CALCULATIONS

	MC1	VS8	MS1	TA1
500 °C				
Activity $NaAlSi_2O_6$	0.97	0.87	0.91	0.94
Activity $NaAlSi_3O_8$ (ordered)[a]	>1	>1	0.76	0.76
Activity $NaAlSi_3O_8$ (disordered)[b]	0.69	0.59	0.51	0.51
ln *K* (ordered)	–	–	−0.19	−0.22
ln *K* (disordered)	−0.34	−0.38	−0.58	−0.61
Pressure (kbar, ordered)	–	–	15.39	15.51
Pressure (kbar, disordered)	16.02	16.20	17.06	17.12
550 °C				
Activity $NaAlSi_2O_6$	0.97	0.87	0.91	0.94
Activity $NaAlSi_3O_8$ (ordered)	0.82	0.70	0.60	0.60
Activity $NaAlSi_3O_8$ (disordered)	0.60	0.52	0.44	0.44
ln *K* (ordered)	−0.17	−0.21	−0.42	−0.42
ln *K* (disordered)	−0.48	−0.51	−0.73	−0.76
Pressure (kbar, ordered)	16.50	16.69	17.59	17.72
Pressure (kbar, disordered)	17.85	17.97	18.93	19.06
600 °C				
Activity $NaAlSi_2O_6$	0.97	0.87	0.91	0.94
Activity $NaAlSi_3O_8$ (ordered)	0.67	0.57	0.49	0.50
Activity $NaAlSi_3O_8$ (disordered)	0.55	0.46	0.40	0.41
ln *K* (ordered)	−0.37	−0.42	−0.62	−0.63
ln *K* (disordered)	−0.57	−0.63	−0.83	−0.83
Pressure (kbar, ordered)	18.60	18.82	19.76	19.81
Pressure (kbar, disordered)	19.51	19.80	20.69	20.72

[a] Microcline model (Bachinski & Müller, 1971); [b]sanidine model (model H1, Hovis *et al.*, 1991); MC 1: Monte Mucrone; VS 8: Val Savenca; MS 1: Montestrutto; TA 1: Tavagnasco. Note: at 500 °C, no pressures could be calculated for samples MC 1 and VS 8 by using the microcline model, since the feldspar compositions are within the solvus and therefore the activity of $NaAlSi_3O_8$ is greater than 1.